Ministry of Higher Education

and Scientific Research

University of Babylon

College of Science for Women

Department of Chemistry

Sonophotocatalytic Study of ZnO and M/ZnO Nanoparticles as a Model of Comparative Study

A Thesis Submitted to the Council of the College of Science for woman, University of Babylon as a Partial Fulfillment of the Requirements for the Degree of Master, in Chemistry

by

Noor Qusay Abdul-Sahib Jassim Bedano

B.Sc., Chemistry of Science, University of Babylon College of Sciences for Women (2018-2019)

Supervised by

Prof. Dr. Ayad Fadhil Alkaim

2022 A.D **1443 A.H**

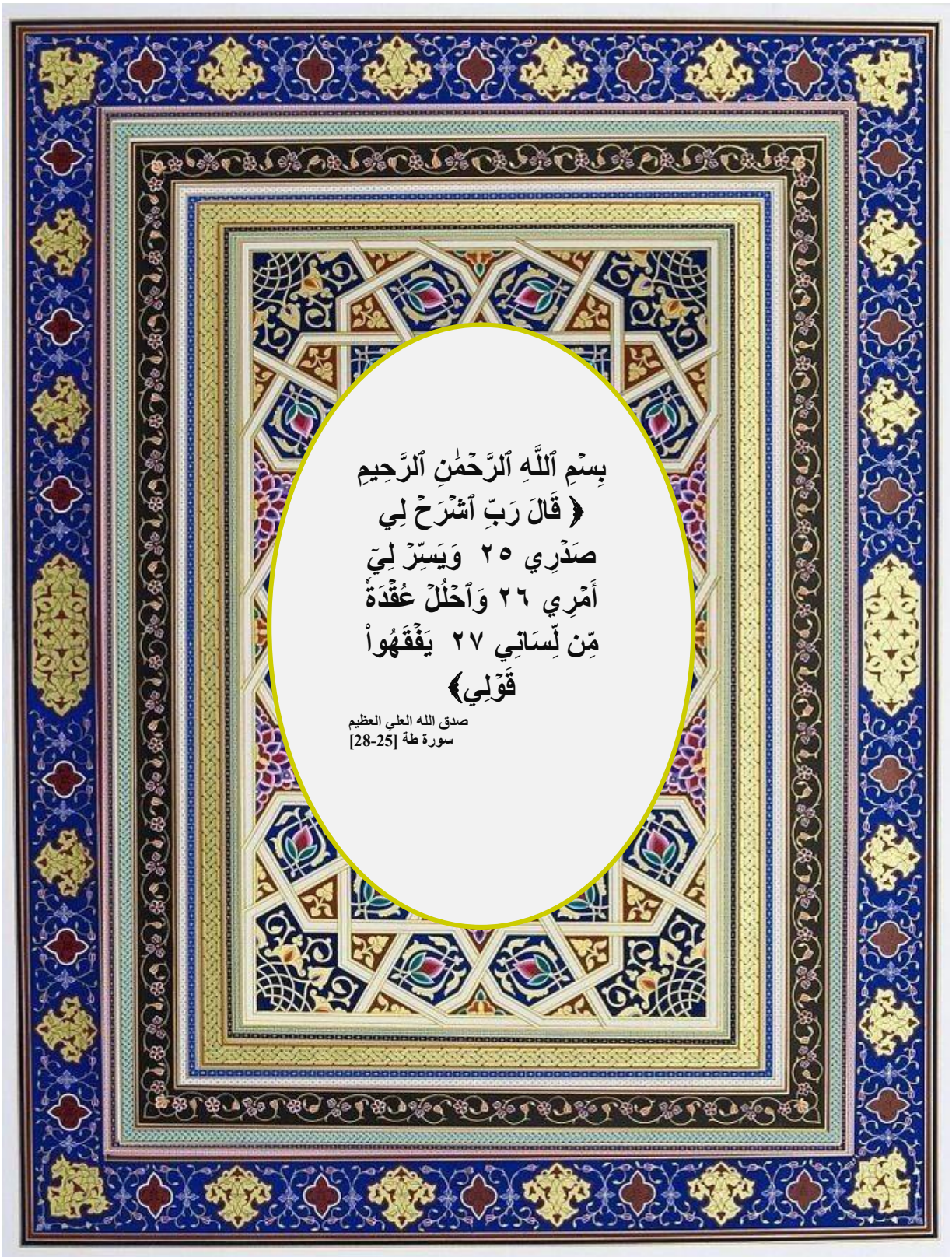
بِسۡمِ ٱللَّهِ ٱلرَّحۡمَٰنِ ٱلرَّحِيمِ
﴿ قَالَ رَبِّ ٱشۡرَحۡ لِي
صَدۡرِي ٢٥ وَيَسِّرۡ لِيٓ
أَمۡرِي ٢٦ وَٱحۡلُلۡ عُقۡدَةٗ
مِّن لِّسَانِي ٢٧ يَفۡقَهُواْ
قَوۡلِي﴾
صدق الله العلي العظيم
سورة طة [25-28]

Certification

I certify that this thesis entitled " Sonophotocatalytic Study of ZnO and M/ZnO Nanoparticles as a Model of Comparative Study" was prepared under my supervision at the Department of Chemistry, College of Science for Women, Babylon University, in partial requirements for the degree of Master of science in chemistry .

Signature:

Name: **Dr. Ayad Fadhil Alkaim**

Title: Prof. Dr .

Address: Department of Chemistry, College of Sciences for

Women, University of Babylon

Date: / / 2022

In the view of the available recommendation, I forward this

thesis for debate by the Examination Committee.

Signature:

Name: **Dr. Hazim Yahya Mohammed Ali**

Title: Assist .Prof. Dr .

Address: Department of Chemistry, College of Sciences for

Women, University of Babylon

Date: / / 2022

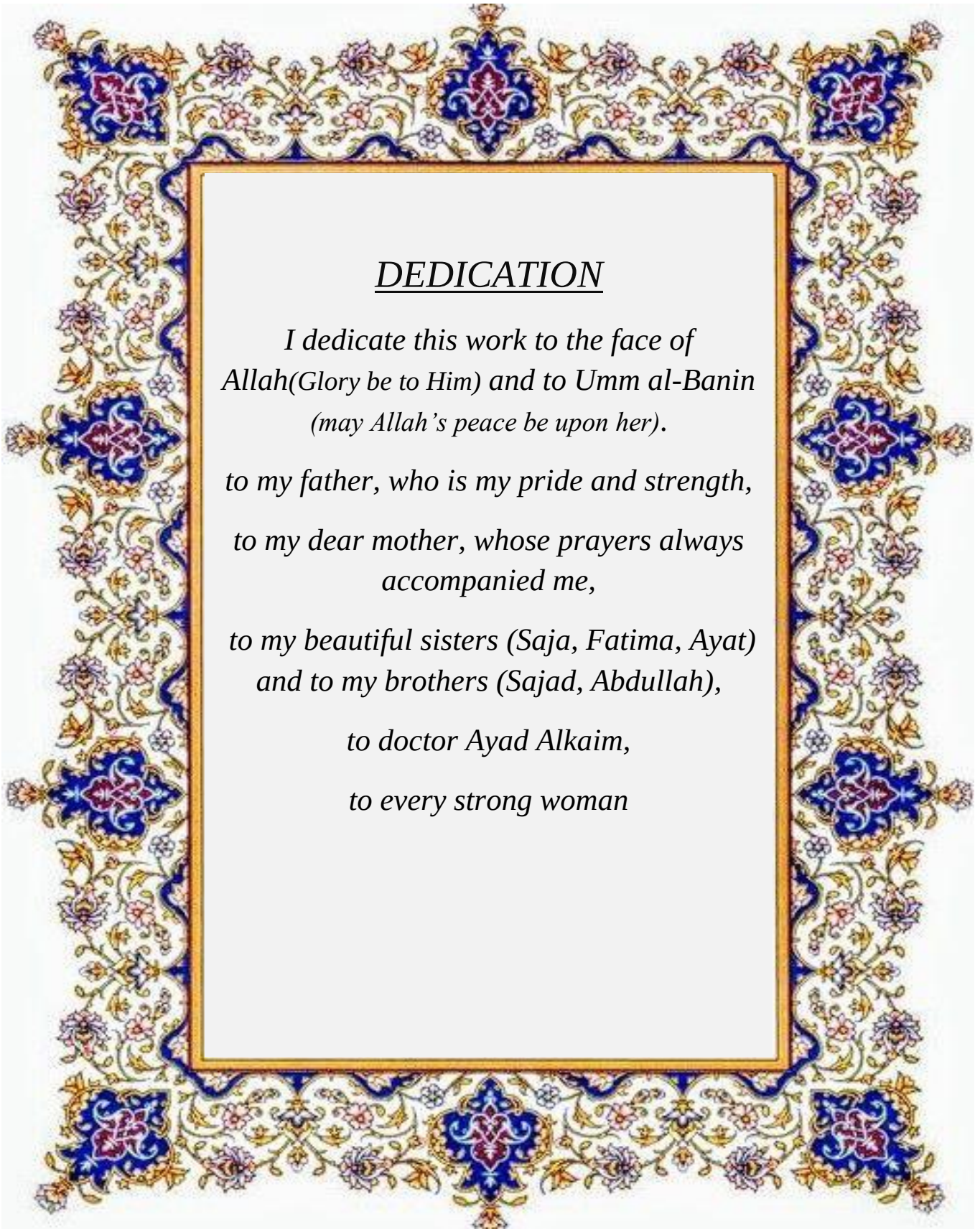

DEDICATION

I dedicate this work to the face of Allah(Glory be to Him) and to Umm al-Banin (may Allah's peace be upon her).

to my father, who is my pride and strength,

to my dear mother, whose prayers always accompanied me,

to my beautiful sisters (Saja, Fatima, Ayat) and to my brothers (Sajad, Abdullah),

to doctor Ayad Alkaim,

to every strong woman

ACKNOWLEDGEMENTS

My first thanks go to Allah (glory be to Him) who enabled me to complete this work and realize my first dream

I extend my sincere thanks to my supervisor Prof. Dr. Ayad Alkaim, for the proposal, guidance and assistance he provided in carrying out this work, It was an honor to be one of his students.

My special thanks and appreciation to everyone who gave me a beautiful words (Dr. Hazim Yahya, *Dr. Dakhil Nasser, Dr. Nour Abdul Razzaq, Dr. Aseel Al-jbore). Thanks to both (Inaam Gouda and Mohamed Salah) for their help and their beautiful and unforgettable situations. I also thank my best friend Lubna Raad, who always listened to me and supported me morally.*

Thank you to all the staff of Department of Chemistry at the College of Science for Woman, University of Babylon .

Finally, I would like to ***thank from the bottom of my heart my beautiful family*** *who is my support in this life and if it were not for your presence, I would not have reached his.*

Abstract

In this study, zinc oxide nanoparticles were prepared using the thermal solvent technique (solvothermal process) at a temperature of 37 °C, at pH 6,the vacuum system and the prepared smaples were incinerated for one hr at a temperature (500 °C). Also, (Ag/ZnO) was prepared by photo deposition using inert environment nitrogen gas .

The chemical and physical properties of the prepared nanocomposites were characterized using different techniques such as X-ray diffraction (XRD), transmission electron microscopy (TEM), scanning electron microscopy (SEM) and UV-visible. Results show doping silver ions on the surface of ZnO, did not show any peaks for Ag in XRD characterization. The UV-visible technology showed that the energy gap of zinc oxide was reduced 3.32 and became less after doping silver 3.31 nanoparticles. The photodegradation of brilliant green dye was studied using ultraviolet light under different conditions in the presence of Ag/ZnO, studying the effect of some factors such as the effect of dye concentration, intensity of incident light and studying the effect of irradiation time.

The results showed that the efficiency of the silver doping zinc oxide surface increased by 92.8%. It also showed that the photocatalytic degradation rate increased with decreasing concentration of brilliant green dye. Increasing the intensity of the light led to an increase in the rate of photocatalytic degradation.

The results of this study showed that the photocatalytic reaction obeys pseudo first order reaction.

List of Continents

List of Figures

List of Table

List of symbols and abbreviations

Symbol	Physical Meanings
C_t	Concentration after different time of irradiation
E.C	Conduction band
e^-/h^+ pair	Electron-hole pair
eV	Electron Volt
E_g	Energy gap
$^*t^{½}$	Estimated half life
FE-SEM	Field emission scanning electron microscop
C_0	Initial Concentration
mW	Milli watt
Nm	Nano meter
NPs	Nanoparticles
$t^{½}$	Observed half life
PDE	Photocatalytic Degradation Efficiency
r	Rate of photocatalytic degradation
hν	The photon energy
TEM	Transmission Electron Microscopes
UV –Vis	Ultraviolet-visible
E.V	Valence band
λ	Wavelength
XRD	X- ray diffraction
ZnO	Zinc oxide

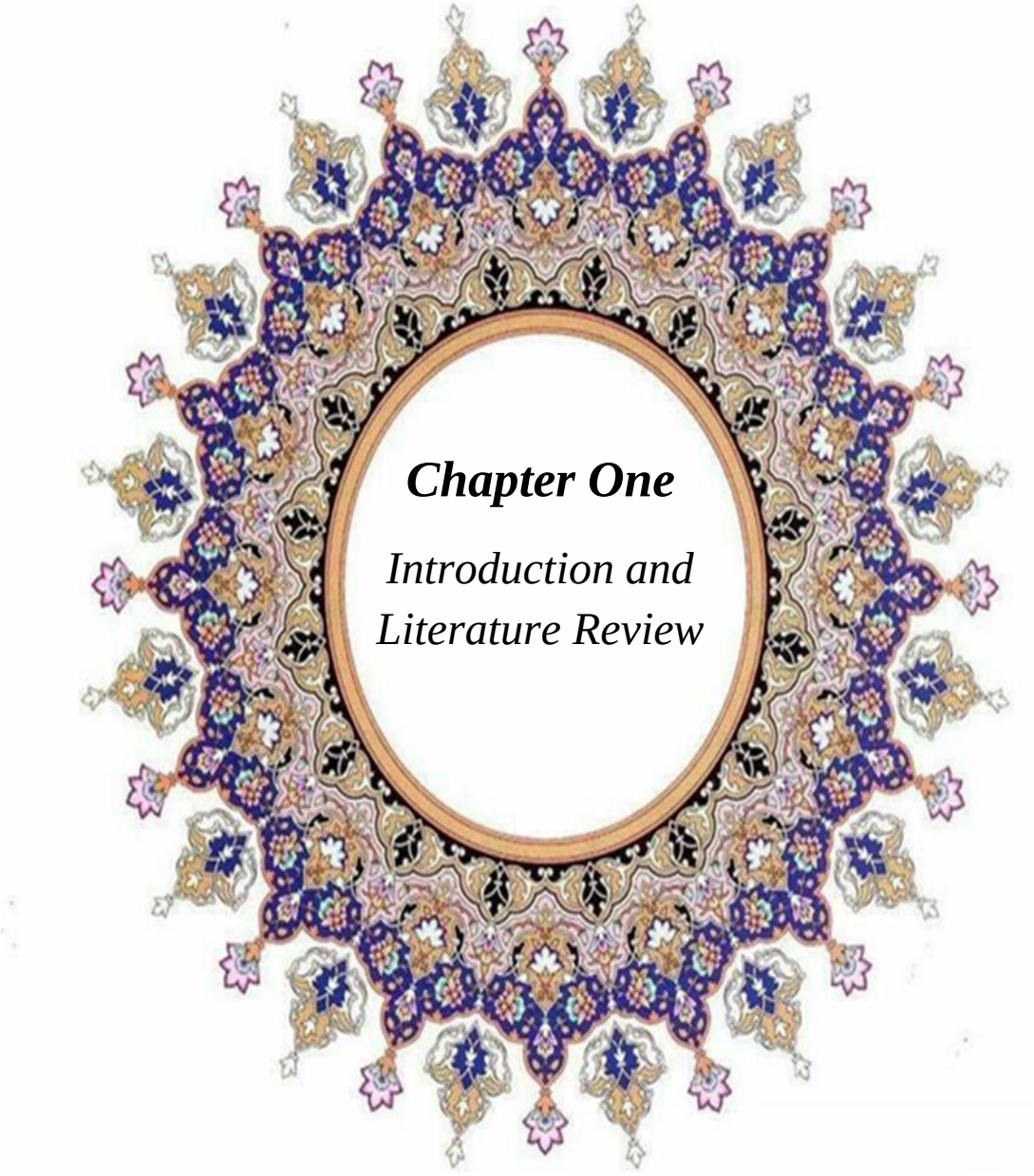

Chapter One

Introduction and Literature Review

1-1 General Introduction

Nanoscience and Nanotechnology (NST) at the dawn of the twenty-first century, a revolutionary research approach to the behavior of matter at the small scale of the nanosystem is revealed. Nanotechnology in Nanoscience (NST) has become a burgeoning field of scientific research and technological innovation over the past two decades at an unprecedented rate. Amazing discoveries, an explosion of new ideas, and endless applications covering a wide range of fields [1].

The term "nanotechnology" was first used by Japanese scientist Norio Taniguchi in 1974 at the International Conference on Micro engineering (ICPE), where it refers to a production technology for obtaining extra high accuracy and ultra-fine dimensions [2].

The term "nano" has become a buzzword and is interesting in relation to modern scientific research. “Nano” is a Greek word meaning dwarf, while in the metric system it means 10^{-9} or one billionth of a metre, because it deals with structures that are very small and invisible to the naked eye, thus providing the ability to create materials, devices, and systems with fundamentally new functions and features [3].

It should be appreciated that nanotechnology is not itself a single emerging scientific discipline but rather a meeting of traditional sciences such as chemistry, physics, materials science, and biology to bring together the required collective expertise needed to develop these novel technologies. This rapid development of nanotechnology and nanomaterials commercially available in the near future raises few concerns about the acute and chronic

toxic effects of nanomaterials that cannot be ignored and need treatment. Therefore, it is necessary to provide an extensive study of the long-term toxicity of nanomaterials use in living system and environmental applications,it is also important to develop robust, environmentally friendly and economical nanomaterials[4].

1-2 Nanomaterials

Nanomaterials and nanotechnology have gained great importance in modern research. One of the first record of nanoparticles in the scientific literature date back to the middle of the 19th century when Michael Faraday was studying gold colloids in the nanometer range [5].

Nanomaterials (NMs) are chemicals or the particles (amorphous or crystalline) that are manufactured and used at a very small scale from 1 to 100 nanometers in at least one dimension. NMs have attracted a lot of attention due to their unique properties. Its importance was realized when researchers found that size affects the physical and chemical properties of a material. Nanoparticles (NPs) show potential for many applications including water treatment plants, oil refineries, petrochemical industries, industrial processes, catalytic processes, buildings, building materials, and diagnostics, and there are several ways to produce NPs, including condensation, corrosion, and culture Ionic, pyrolysis and hydrothermal synthesis [6].

The nanomaterials showed various combinations of nanoparticles, metallic NPs, metal oxide nanoparticles, semiconductor NPs, carbon-based NPs (fullerene, graphene, carbon nanotubes (CNT), carbon nanofibers,

carbon black), polymeric NPs and more where a small selection is displayed in Figure (1-1) [7].

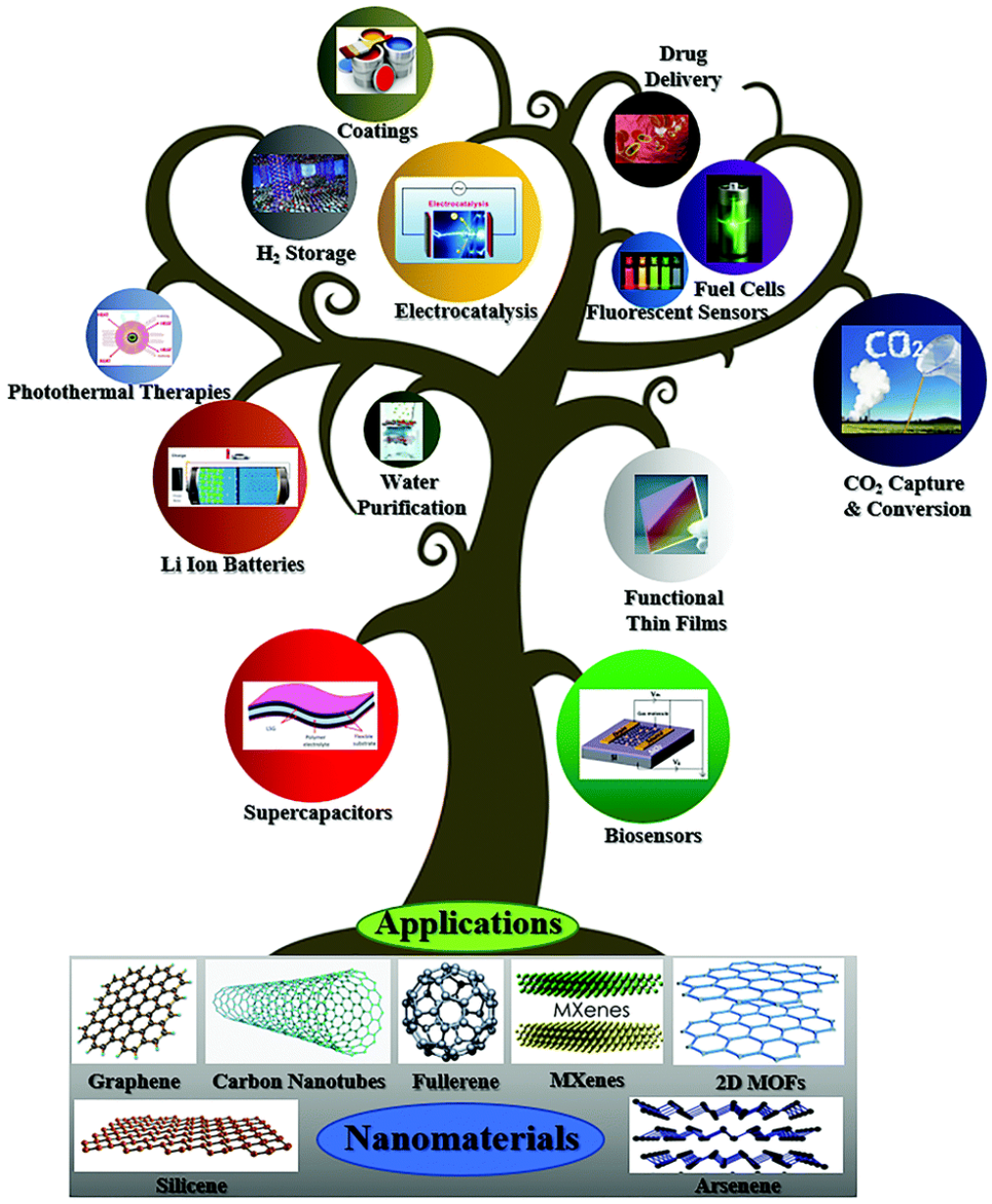

Figure (1-1): Types of Nanomaterials and Their Applications [8].

1-3 Classification of Nanomaterials

During the past decade, nanomaterials have been classified into different groups based on different criteria. The idea of the first classification of nanomaterials was introduced by Gleiter in 1995, and explained by Skorokhod in 2000[9]. They are classified according to their dimensions, morphology, state and chemical composition, this classification is also based on their size, which ranges from 1 to 100 nanometers in at least one the dimension . Based on their overall dimensions and shape for this material, NMs can be divided into four classes[10] **:**

1. **Zero-dimensional (0D)** nanomaterials possess all dimensions at the nanoscale, i.e. the size is less than 100 nm. 0D includes spherical, cube, polygonal nanometer, hollow sphere, metallic.
2. **One-dimensional (1D)** nanomaterials are materials with one dimension not at the nanoscale while the other is two dimensions at the nanoscale. 1D includes metallic, polymeric, ceramic, nanotube, ,nanorod filament, nanowires and nanofibers.
3. **Two-dimensional (2D)** nanomaterials only one of the dimensions is located on the nanoscale while the other two are not. 2D includes thin films, nanosheets, and monolayer (crystalline or amorphous nanolayers).
4. **Three-dimensional (3D)** nanomaterials have various dimensions exceeding 100 nm . (3D) NMs combine multiple nanocrystals in different directions. Examples include foams, fibres, carbon nanotubes, fullerenes, pillars, polycrystalline, honeycombs, and layered structures [11].

1-4 Synthesis Method of Nanomaterials

There are different methods and techniques for the synthesis of nanostructured materials, which have been classified on the basis of the processes involved in constructing nanostructures into two approaches: bottom-up and top-down approaches (see Figure. 1-2).

In the bottom-up approach, the NPs are first obtained at the atomic level and then incorporated into the desired material. This includes the formation of NPs from colloidal dispersion and the formation of powders by the sol-gel method, which is then followed by integration. Other examples include deposition, reduction, green synthesis, spinning, biochemical synthesis, atomic layer deposition, molecular self-assembly, and vapor phase deposition.

In the top-down approach, bulk materials are cut at the microscopic level into the required NPs by various means. Some examples are etching, ball milling, milling/milling, CVD, physical vapor deposition (PVD) and optical lithography, etc [12, 13].

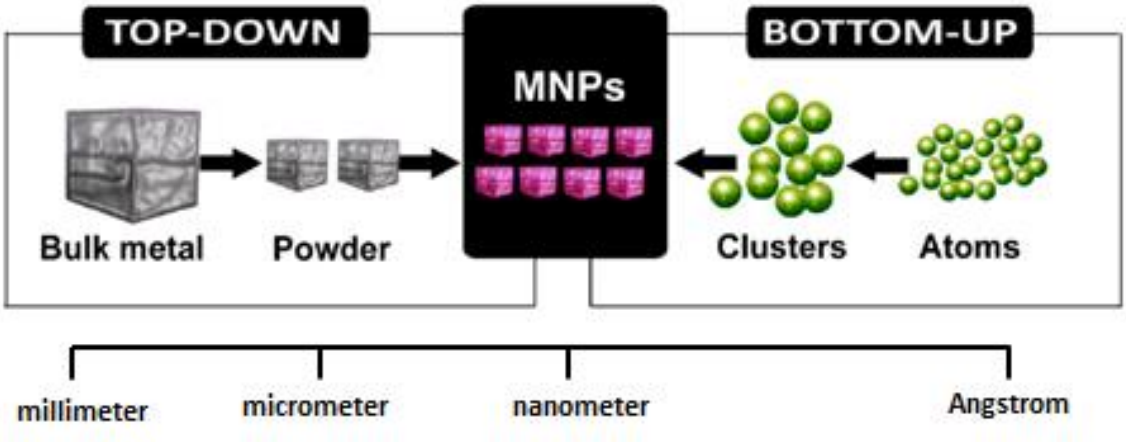

Figure (1-2): The top-down and Bottom-up Methods for Nanoparticle Preparation[14]

1-5 Crystal Structure of Zinc Oxide

ZnO is one of the most significant nanomaterials that has been widely studied for many decades, generally, ZnO crystallizes in three forms hexagonal Wurtzite ,cubic zinc blende and cubic rock salt as in Figure (1-3). It is obtained only at optimum pressure and temperature. The crystal structure is composed of two interpenetrating hexagonal-close - pack (hcp) sublattices [15].

One sub-lattice consists of four O^{2-} and Zn^{2+} ions in one unit cell forming a tetrahedron structure sp3 covalent bonding. The strongest polarity surfaces are due to the positively charged for 0001 - zinc polar surface and negatively charged for 0001 - oxygen polar surface. The two important features of the Wurtzite structure are the polar surfaces and noncentral symmetry. When a stress force is applied, the non-central symmetric

structure will due to the separation of the central point of negative charges and that of positive changes leads to a temporary polarization [16].

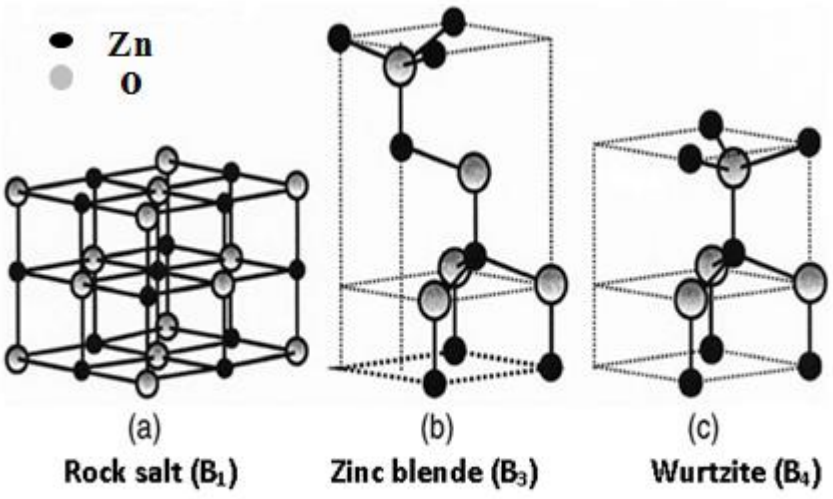

Figure (1-3): Crystal Structures of zinc oxide [17]

1-5-1 The Properties of Zinc Oxide

ZnO is one of the most promising materials that has received special attention among various metallic semiconductor materials, which finds a large number of technological applications, due to its unique properties, including optical and thermal stability, excellent low toxicity, physical and chemical stability and abundance [18].

ZnO is a II-VI metal oxide that is white in color and insoluble in water, has a wide direct band gap energy (3.37 eV) slightly greater than TiO2 (3.0-3.2 eV), high electron binding energy (60 meV) [19] .In the table (1-1) are the basic properties of zinc oxide. This wide band gap energy allows ZnO to absorb UV light at ~370 nm, generating excitons that can be harnessed for solar and photocatalysis applications. The large exciton binding energy of

ZnO means these excitons are stable at room temperature. Without this binding energy, the electrons and holes would recombine too quickly to be of practical use. The high photosensitivity and wide band gap of ZnO allow oxidation and reduction reactions to be carried out on the ZnO surface by the holes and electrons generated by UV absorption[16].

Zinc oxide shows a strong n-type conductivity with electrons to They move in the conduction band as charge carriers . But the source of this conductivity is still under discussion [20], this is mainly due to a large number of original deffects such as oxygen vacancies, zinc vacancies, oxygen interstitials, and zinc interstitials .These oxygen vacancies have the formation lowest energy and are thus the easiest to form. Obtaining p-type doping in ZnO is a very difficult task. One reason is that ZnO has a tendency toward n-type conductivity ,this problem is also seen with other III–V and II–VI wide bandgap semiconductors—almost all of which are easy to dope n-type but much harder to dope p-type. In this respect, the only major exception appears to be ZnTe [21], which is quite easy to dope p-type. That the conductivity in ZnO samples is very sensitive to modifications on the surface due to annealing in different environments. Moreover, very little is known about the surface states in ZnO, and comprehensive investigations on controlled ZnO surfaces are still needed in order to assess the potential formation of the surface electron accumulation layer and its effects on electrical measurements. Recently, ZnO nanostructures have been studied as conductive compounds in polymers with high electrical permittivity, and they have received increasing attention for their potential application in high charge and storage capacitors[22].

One of the fascinating features of ZnO crystal is anisotropic growth, which enable the easy fabrication of 1D nanowires or nanorods structures as compared to nanoparticles. The electronic properties of hexagonal ZnO have been investigated by applying various approaches, such as local density approximation (LDA) to find out its band structure. LDA have confirmed the position of VB between ⁻10 and ⁻5 eV corresponds to the Zn-3d levels while the upper bands from ⁻ 5 to 0 eV corresponds mainly to O-2p orbitals. It is important to mention here that, empty Zn-4s levels constitute two bands in the CB of ZnO and hence the band gap can be calculated from these band positions [23].

ZnO nanostructures can be fabricated by chemical, physical or green approach, With increasing awareness on environmental issues, green synthesis has emerged as a desirable method as it aims to produce nanomaterials with none or minimum usage of hazardous chemicals. Instead, different biological sources from plants, fruits, microbes and biopolymers are utilized during green synthesis process. A wide range of techniques including hydrothermal process, microwave decomposition, precipitation and wet chemical method has been adopted to produce ZnO nanostructures of different morphologies . Published works have reported successful ZnO nanostructures production of spherical , flower , thorn-like and rods shapes [17] .

Table(1-1): Basic Properties of Zinc Oxide[24]

Parameter	Value
Bandgap	3.37 eV (direct bandgap)
Density	5.606 g. cm^{-3}
Crystal structure	Wurtzite, rock salt and zinc blende
Stable phase at 300 K	Wurtzite
Appearance Amorphous	Amorphous white or yellowish white powder
Melting point	1975ºC
Nature of oxide	Amphoteric oxide
Exciton binding energy	60 meV
Ionicity	62%
Refractive index	2.0041
Solubility in water	0.16 mg 100 ml^{-2}
Relative dielectric constant	8.66
Lattice constants at 300 K	a : 0.32495 nm c : 0.52069 nm

1-5-2 Synthesis of Zinc Oxide

The zinc Oxide is synthesized by adopting different strategies, Such as solution-based synthesis and vapor-phase-based methods. It is worth noting here that synthesis methods can have a significant impact various parameters, such as particle size and crystallization. The solution-based synthesis methods are preferred for controlling the morphology and size of nanostructures by changing the solvent, precursor and reaction conditions, such as temperature, heating time, etc . The following are the main methods of synthesis of zinc oxide.

1-5-2-1 Hydrothermal Method

The hydrothermal method is a type of soft chemical synthesis method developed by simulating the formation process of some ores in nature. The hydrothermal method refers to the use of an aqueous solution as a reaction system in a special closed reaction vessel to create a high temperature, high-pressure reaction environment by heating the reaction system and pressurizing it (or the vapor pressure generated by itself). The process dissolves and recrystallizes a substance that is poorly soluble or insoluble under normal conditions [25]. Number of features make hydrothermal synthesis an ideal method for preparation of nanoparticle. The resulting nanocrystals are empty defect-free with high specific surface area, low agglomeration between particles, good crystallinity, high product purity, crystal symmetry, narrow particle size distribution, formation of anatase at relatively low temperature (< 200 ˚C), low energy consumption, and inexpensive instrumentation [26] .

1-5-2-2 Solvothermal Method

Solvothermal synthesis is a method similar to hydrothermal synthesis but involves organic solvents instead of water. In comparing to other methods, solvothermal synthesis has several advantages, solvothermal conditions are permit rapid convection in solution [27]. The comparably mild environment offers conditions to form crystals with few lattice defects and it allows for the precise control over the size, shape distribution, and crystallinity of nanoparticles. The low boiling point of organic solvent involved can provides a higher reaction pressure when proceed at high temperatures, which will contribute to the procedure of crystallization, Because of the mild temperature, special structural features of precursors can be transferred to the products so that the morphology of products can be controlled. Solvents can also provide functional groups, which can further react with the precursors or the products to synthesize novel materials. solvothermal synthesis can reduce the releasing of harmful vapour during the reaction. The sealed system not only contributes to carry out green chemistry, but also efficiently reduces the possibility of oxidation and contamination from atmosphere or oxygen, an important point for high purity products. Finally, in order to control the size as well as the shape of nanoparticles synthesized [28].

1-5-2-3 Sol-gel Method

The sol-gel process also recognized as chemical solution deposition is a wet chemical technique. In this method, a precursor such as a metal alkoxide or an inorganic compound is hydrolyzed under certain conditions to

form a stable and transparent sol system, and then poly condensed into a gel, finally dried, sintered and solidified to form a solid. In this method Widely used due to cost : (1) low reaction temperature and easy control of the reaction; (2) high uniformity and purity of the sample, uniformity up to the molecular or atomic level; (3) accurate stoichiometry, easy modification, the wide doping range. The sol-gel method plays an important role in soft chemical synthesis [29].

1-5-2-4 Precipitation Method

Precipitation method can be defined as a chemical reaction occurring in an aqueous solution where two ionic bonds combine, resulting in the formation of an insoluble salt . These insoluble salts formed in precipitation reactions are called precipitates. Precipitation reactions are usually double displacement reactions involving the production of a solid form residue called the precipitate. These reactions also occur when two or more solutions with different salts are combined, resulting in the formation of insoluble salts that precipitate out of the solution [30].

1-6 Photocatalytic degradation

Photocatalysis is a reaction which uses of near ultraviolet light ($\lambda < 380$ nm) to excite a semiconductor photo catalyst in the presence of oxygen, in which the photo catalyst modifies the reaction without consumed as a reactor. Type and size of photo catalyst has major influence in photocatalysis. Band gap energy to activate the catalyst should be correlated with the wavelength of light source. As size decreases, the specific surface area of photo catalyst illuminated and contact area of photo catalyst with

reaction medium increases [31]. Muller reported in 1969 that ZnO could decompose isopropanol under UV light . This discovery demonstrated the potential of photo catalysts to degrade organic substances in water. Since then numerous scientists devoted their time and effort to research in the photocatalytic field improving photocatalytic efficiency, and expanding the range of photocatalytic systems and applications [32]. Semiconductors are known as the most important photo catalyst materials which possess a valence band (with full electron) and a conduction band (with higher energy and no electron) with definite band gap. The basic mechanism of the photocatalytic process is when photons of a light source with energy (hν) greater than or equal to the band gap energy (Eg) of ZnO catalyst shine on it, electrons get excited from the valence band (VB) to the conduction band (CB) region, leaving holes in the VB. This creates electron hole (e^-/h^+) pairs, as shown in Figure(1-4).

$$\mathbf{ZnO + h\nu \rightarrow ZnO\ (e^-/h^+)} \qquad \mathbf{(1\text{-}1)}$$

Dye molecules absorb photons and get energetically excited from their highest occupied molecular orbital (HOMO) to lowest unoccupied molecular orbital (LUMO) .

$$\mathbf{Dye + h\nu \rightarrow Dye^*} \qquad \mathbf{(1\text{-}2)}$$

Then, the photo excited electrons diffuse on to the surface of the catalyst and react with adsorbed oxygen, reducing it to superoxide radical ion (O_2^-) .

$$\mathbf{e^- + O_2 \rightarrow O_2^-} \qquad \mathbf{(1\text{-}3)}$$

Then oxidized to cationic radicals dye^+. By injecting their LUMO electrons to the CB of the semiconductor or to oxygen dissolved in solution .

$$\mathbf{Dye^* + O_2 \rightarrow O_2^- + Dye^+} \qquad \mathbf{(1\text{-}4)}$$

while the holes move to the surface and react with neighboring adsorbed H2O or dye molecules, oxidizing them to hydroxyl radical ($OH^{\bullet}$) .

$$\mathbf{H_2O + h^+ \rightarrow OH^{\cdot} + H^+} \qquad \mathbf{(1\text{-}5)}$$

and oxidized dye radical cation (dye^+).

$$\mathbf{Dye + h^+ \rightarrow dye^+} \qquad \mathbf{(1\text{-}6)}$$

It is mainly due to the formation of the reactive hydroxyl and superoxide radicals in the solution that set in a chain of catalytic reactions leading to the eventual degradation of the dye in to CO_2, H_2O, and few mineral acids .

$$\mathbf{Dye + OH^{\cdot} \text{ or } O_2^- \rightarrow \text{Degraded products}} \qquad \mathbf{(1\text{-}7)}$$

The redox reactions of the (e^-/h^+) pairs on the surface of ZnO catalyst play an essential role in their separation and hence enhancing the rate of degradation. However, fast recombination lowers formation of radicals and decreases rate of degradation. The presence of oxygen in the solution as a scavenger for the excited VB electrons and surface defects on ZnO catalysts, acting as trapping centers for holes and electrons prevent pair recombination and can maximize rate of degradation[33, 34].

Used nano-semiconductors including TiO2, ZnO, SiO2, Fe2O3, CdS, ZnS, etc increasingly to satisfy some environmental issues by several applications

such as solar cells, water splitting, sensors, and so forth. Some necessary properties of semiconductors are (i) photo responding, (ii) being stable in terms of chemical, biological and light corrosion, (iii) high activity in the UV-vis region, (iv) cheapness, and (v) no toxicity. Compared to the other methods [35, 36].

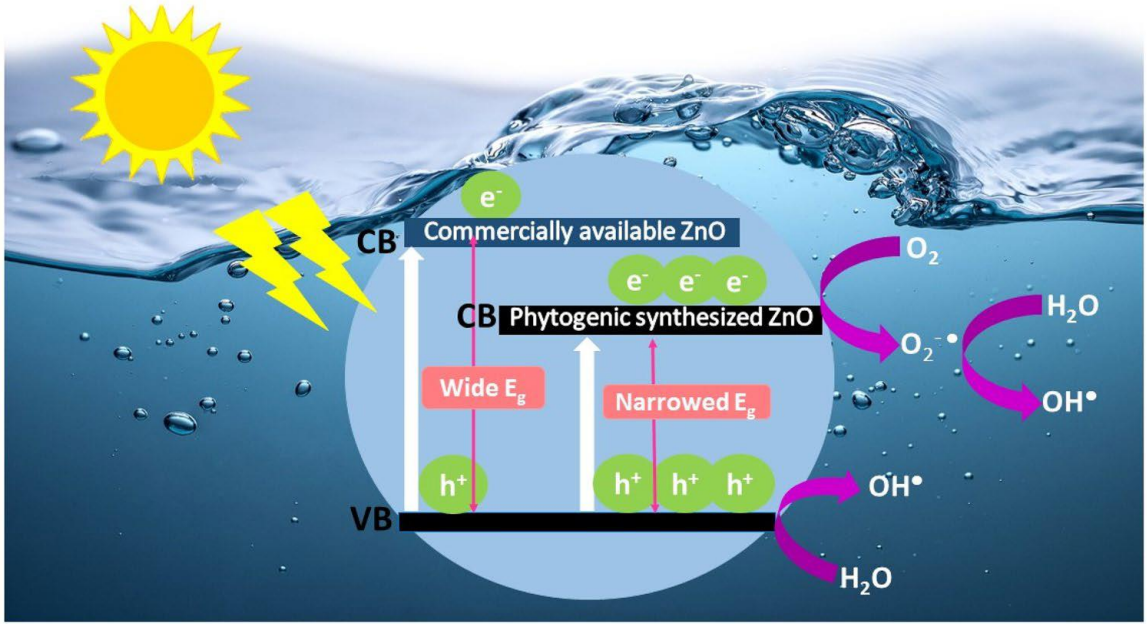

Figure (1-4): Mechanism for Photocatalytic Degradation of Dyes[37]

1-7 M/ZnO Nanoparticle

The zinc Oxide shows low efficiency under solar radiation due to its wide bandgap and fast electron-hole recombination. Noble metal nanoparticles, such as Pd, Pt, Au, and Ag, are introduced onto the surface of

ZnO which enhances the photocatalytic reaction in the decomposition of various organic dyes [38, 39]. Among noble metals, metallic silver nanoparticles exhibit high efficiency in enhancing the photocatalytic activity of ZnO because of their appropriate price in comparison with other noble metals such as Au, Pt, and Pd . The enhanced UV-light-driven photocatalytic efficiency was attributed to efficient separation of the photogenerated electrons and holes in the presence of Ag ; however, the higher visible-light-driven photocatalytic efficiency was attributed to surface Plasmon resonance of Ag. It is interesting to mention that the existence of an appropriate amount of metallic silver nanoparticles is a major factor in optimizing the photocatalytic reactivity[40]. A small amount of Ag ° is not sufficient to enhance the reactivity; however, a large amount of silver metal acts as recombination centers that prevent the production of a large amount of radicals and reduce the lifetime of the photo catalyst. The homogeneous dispersion of metallic silver nanoparticles on the ZnO surface requires a mild reduction process; however, most of the previous research work usually used a vigorous reducing agent such as $NaBH_4$, ascorbic acid, or $LiAlH_4$. These strong reducing agents lead to agglomeration of silver nanoparticles on the ZnO surface, which inhibits light penetration and results in the silver nanoparticles acting as recombination centers for the charge carriers[41, 42].

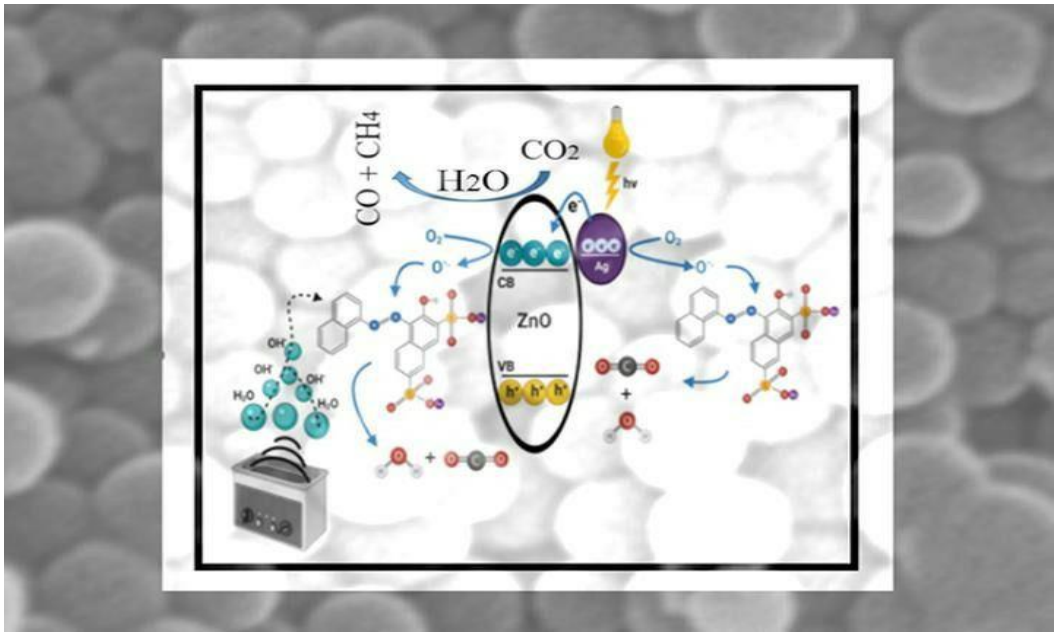

Figure (1-5): Mechanism of M/ZnO Nanoparticle for Photocatalytic Degradation of Dyes

1-8 Literature Review

- **Jing et al. (2001).** They used different techniques such as TEM, XRD, BET, SPS, EPR, IR and XPS to study the surface properties of ZnO nanoparticles (UFPs) prepared by pyrolysis of zinc hydroxide precursors. They found that there are surface-active species that improve photocatalytic activities such as hypoxia and hydroxylation. The concentration of these active species decreases with the increase in temperature, surface area and photovoltaic cells, and the photocatalytic activity of the molecules will decrease with the increase in their size, which means that these activities depend mainly on the properties of the surface [43].

- **Kinuyo Kawano et al. (2002)** Their research involved studying the optical absorption of the Ag ion on a single crystal surface of ZnO, which was prepared by a hydrothermal process. Their results showed that the surface reaction of the Zn electrode was higher than that of the polar O surface , but there was less photodegradation at Zn compared to the polar O surface . Where The Ag ion in aqueous solution was rapidly on the surface of a low ZnO single crystal under UV irradiation [44].
- **P.S. Xu et al. (2003)** They calculated the electronic structure of ZnO and its defects, which included intrinsic point defects and their complexes. According to their calculation data, the positions of the defect state levels have been determined in the energy band of ZnO [45].
- **Jing Liqiang et al. (2004)** . That ZnO can be nearly inactivated in the gas phase photocatalytic oxidation of n-C_7H_{16}. It is also possible to the photocatalytic oxidation of ZnO to be deactivated. The inactivation was mainly caused by the change of the surface conduction type of the N-type semiconductor before the P-type photocatalytic reaction after the inactivation due to the adsorption of oxidation products such as H_2O, CO_2, and SO_3 on the surface of the semiconductor photocatalyst. In addition, the inactivated photocatalyst can be regenerated almost completely by washing and drying **[46].**
- **Chin-Cheng Hsu et al. (2005),** They synthesized ZnO/ZnO_2 composite photocatalysts were synthesized by hydrothermal treatment at 120–180 °C of ZnO_2, which in turn was obtained from an aqueous solution of $ZnSO_4$ and H_2O_2. The synthesized particles showed the shape of prismatic ZnO crystals with small “fused” ZnO_2 grains on the surface. This study demonstrates a novel approach to synthesize a composite photocatalyst

containing strongly coupled components through phase shift reactions between the components **[47].**

- **Murray J. Height et al. (2006).** They made Ag-ZnO catalysts with a high surface area by flame spray pyrolysis (FSP). They obtained silver metal clusters deposited directly on ZnO nanocrystals from this process, used photolysis of 10 ppm methylene blue (MB) solution to evaluate the performance of FSP-made Ag-ZnO and were compared with wet Ag-ZnO and reference titania photocatalysts. The optimum photolysis rate for Ag loading was about 3 at .% [48].
- **Vladimir K. Ivanov et al. (2007).** They developed new methods for the synthesis of high-dispersion ZnO powder based on microwave heating of salt mixtures as well as microwave-assisted low hydrothermal treatment of zinc hydroxide. It was found that the obtained powders possessed high photocatalytic activity **[49] .**
- **Tian Tan et al. (2008)** In this two-step method for the photo catalyst synthesis of a heterogeneous structure of a metal semiconductor is presented, which is based on tetrapod-like zinc oxide (T-ZnO) precipitated by thermal evaporation. The Ag/T-ZnO heterostructure prepared by the RF magnetron spraying method shows better photocatalytic activity than that of pure T-ZnO. The improved photocatalytic activity indicates the feasibility of this new two-step method that can be developed for a promising synthesis technique [50].
- **Matin Sadat Mohajerani et al. (2009)**, The effect of the shape of ZnO nanostructures prepared by hydrothermal method on photo activity was studied. The nanorods were found to be slightly higher than the 3D

flower-like and microscopic nanostructures. As no direct relationship can be established between crystal size and photoactivity [51].

- **Dapeng Wu et al. (2010) .**ZnS porous tubes comprising 10 nm nanocrystals were fabricated as a photo catalyst using ZnO rods as a template. ZnO rods were first synthesized in aqueous solution and poly(vinylpyrrolidone) played a major role in the diameter processing. Then, Na2S solution was used to convert the ZnO rods into porous ZnS tubes. According to time-dependent experiments, the dissolution of the inner ZnO core is subject to the anisotropic habit of the ZnO crystal. The as-obtained ZnS porous tubes show a broad and strong UV absorbance around 350 nm and possess good photocatalytic efficiency in decomposing rhodamine B under UV irradiation **[52].**
- **M. Qamar et al. (2011) .**The present study demonstrates the complete removal of Cr(VI) in aqueous suspensions of zinc oxide nanoparticles using a novel laser-induced photocatalysis process without the use of any additive. The study showed that ~95% Cr(VI) was removed within a short time (60 min) of laser exposure in the presence of ZnO. However, the removal of chromium using the conventional setup under similar conditions was found to be negligible [53].
- **Tania R. Girardi et al. (2012)** This paper describes the development of crystalline ZnO particles by chemical method, using three different precursor salts and two different synthesis methods: precipitation and citrate method. Rhodamine B (RhB) degradation was used as a probe reaction to test the ZnO photosynthetic activity of the complex. It has been observed that crystallization and surface availability, correlated with the presence of synthesis residues, are the primary factors for

determining photosynthetic activity. On the other hand, the surface area, agglomeration and degree of sintering, which are actually affected by the composition course and antagonisms, do not play any significant role in it. The deposition method appears to be most suitable for the synthesis aimed at photolysis. Regarding the characteristics of the sample, crystallization becomes the most relevant factor to explain the photosynthetic activity of the samples [54] **.**

- **Ang Wei et al. (2013)** A graphene-ZnO (G-ZnO) hybrid was fabricated by one-step electrochemical deposition. During the formation of a ZnO nanostructure by cathodic electrochemical deposition, the graphene oxide was electrically reduced to graphene simultaneously. More importantly, it showed exceptionally higher photocatalytic activity for the degradation of methylene blue dye than that of pure ZnO nanostructure under both UV and sunlight [55].
- **Lun Pan et al. (2014)** The abundant zinc vacancies (7.5 mol) were successfully introduced into unsaturated ZnO by a simple thermal melting method followed by thermal calcination. The presence of Zn vacancies led to some new properties in ZnO, such as p-type conductivity, room temperature ferromagnetism, and high photocatalytic activity. This work demonstrates that metal defects can be easily engineered in non-clad metal oxides, which may lead to many unexpected behaviors and thus broaden the compositional approach and application of functional materials in energy fields **[56] .**
- **JoydebManna et al. (2015)** The growth of metal domains on semiconducting nanoparticles is known to enhance their photocatalytic properties. They prepared ZnO nanoparticles decorated with metallic

Au domains by a novel single-pot microwave-based strategy. The industrial route used microwave heating of a mixture of only three ingredients: zinc ions. We showed that the hybrid Au/ZnO nanoparticles exhibited improved photocatalytic properties compared to regular ZnO nanoparticles [57].

- **Delei Ding et al. (2016)** Compound zinc/carbon oxide nanoparticles (CQDs) have been successfully synthesized by an easy process. It was found that the ZnO foam consists of a large number of ZnO nanoparticles that fill the irregular pyramidal pores. The synergistic effect is attributed to several factors, including the light-trapping effect of the ZnO foam, the up-shifting photoluminescence behavior and the photo-induced electron transfer property of the copious quantum dots [58].
- **Minh Tan Man et al. (2017)** They report a chemical bath deposition approach for preparing large arrays of ZnO nanostructures. Photoluminescence dynamics showed that many of the visible emission characteristics are related to defects such as oxygen vacancy, zinc interstitial, or their complexes. In addition, the precipitated ZnO nanorods showed excellent performance in adsorption and photodegradation of organic dyes, achieving 95% of photolysis. Moreover, oxygen defects act as trap sites with strong adsorption capabilities towards organic dyes and showed high performance in photolysis of dye molecules [59].
- **Salimeh Kimiagar et al. (2018)** They prepared naked and N-doped (NrGO) graphene samples using the hydrothermal method. All near-band photoluminescence emissions for the samples started at about 380 nm (at 3.26 eV). Interestingly, we observed a slight improvement in the electron capture effect of graphene by doping nitrogen into its substructure. This

behavior can be appropriately used to rescue the photogenerated electrons on the ZnO surface [60].

- **C.A. Soto-Robles et al. (2019)** This work evaluates the effects of different concentrations of extracts of the hibiscus flower (Jamaica) on the green synthesis of zinc oxide (ZnO). Zinc nitrate was used for the synthesis of ZnO as a source of zinc ions. 1%, 4%, and 8% (wt.%) of hibiscus extracts, in aqueous medium, were used as reducing and stabilizing agents in the characterization of FTIR, Znsingle bond binding was observed at 618 cm-1. By means of XRD, the material is observed to have a hexagonal crystal phase (Wurtzite). Through XPS, energy values of 1022eV for Zn and 531eV for O are observed, illustrating the chemical state of Zn+2. The shape of ZnO nanoparticles (NPs) varies in their semicircular shape and size distributions depending on the extract used, which ranges from 30 to 8 Nm. The band gap values decreased from 2.96 to 2.77 eV with increasing concentration of the extract. These materials presented good photocatalytic activity, decomposing 97% of methyl bromide in 150 min, which are similar effective results to green ZnO NPs synthesized via other extracts and methods[61].
- **Chuansheng Chen et al. (2020)** To improve the catalytic activity of the ZnO nanostructure in natural sunlight, they used SnO to sensitize the ZnO nanostructure, the resulting SnO/ZnO nanostructure showed very high catalytic activity and catalytic stability under natural sunlight irradiation. Moreover, the introduction of SnO could confer ZnO 's ability to photodegrade in the dark. The improved photocatalytic performance is mainly attributed to the positive synergistic effect between ZnO and SnO. This work contributes to the design of other photo catalysts derived from

visible light for application in environmental purification of organic pollutants [62].

- **Marie Le Pivert et al. (2021)** This work aims to develop civil engineering materials that are employed through direct growth of ZnO nanostructures as a more environmentally friendly and biocompatible approach to reducing air pollution. By scaling up an innovative and low-cost direct hydroponic growth synthesis, a few square meters paved slabs and bitumen road were easily produced for large-scale evaluation of their photocatalytic activity under a solar lamp in a climate chamber. Bitumen is responsible for the emission of pollutants [63].
- **Ashkan VakilipourTakaloo el al. (2021)** An oxide/metal/oxide multilayer electrode is employed to improve the mechanical flexibility as well as power conversion efficiency of organic photovoltaics. However, its performance needs to be further improved to provide a higher conversion efficiency and better environmental compatibility with curved indoor electronics. In this study, ZnO/Ag/ZnO nanomesh electrodes are incorporated into the inverted non-fullerene organic photovoltaics to enhance the efficiency under indoor and outdoor lighting illumination in a flexible mode. The opto-electrical properties of the perforated ZnO/Ag/ZnO nanomesh electrode with different hole sizes are compared with those of the planar ZnO/Ag/ZnO and indium tin oxide electrodes. The micro-cavity effect and haze effect, which plays a crucial role in determining the performance of the organic photovoltaics, are directly related to the hole diameter. Despite higher transmittance of indium tin oxide, organic photovoltaics using ZnO/Ag/ZnO nanomesh electrodes with a hole diameter of 350 nm exhibits an average conversion efficiency

of 15.7% under a 1000 lux light-emitting diode lamp; this efficiency is 45.3% and 27.6% greater than those of organic photovoltaics using indium tin oxide and planar ZnO/Ag/ZnO electrodes, respectively. Furthermore, all ZnO/Ag/ZnO nanomesh-based organic photovoltaics show much higher mechanical flexible properties than those of the planar ZnO/Ag/ZnO-based organic photovoltaics**.**

- **Muñoz-Fernandez et al. (2022).** In this present paper, Ag/ZnO-based nanostructures with aspect ratios ranging from 5.9 to 11.4 have been successfully obtained. The photocatalytic behavior was improved by incorporating silver nanoparticles into ZnO nanowires. Moreover, results of close to 100% decomposition were obtained for a sample synthesized with an average reaction time, a high Ag^{+}/Zn^{+} ratio, and in the presence of a dispersant, demonstrating that these were the optimal operating conditions. Therefore, Ag/ZnO-based PCA nanostructures depend on crystallinity, surface area, and particle morphology, which are also highly dependent on the synthesis conditions[64].
- **L.Muñoz-Fernandez et al . (2022).** This study presents the advances in the field of ZnO/Ag catalysts from the synthesis of hierarchical ZnO nanowires (NWs) decorated with Ag nanoparticles, prepared by a facile solvothermal method at 120°C. It evaluates the photocatalytic efficiency from studying the time reaction of Ag/Zn concentration ratio and the presence of cetyltrimethylammonium bromide (CTAB) as an organic dispersant. X-ray diffraction, scanning electron microscopy, and analytical/high-resolution transmission electron microscopy results confirmed the presence of homogeneous cylindrical ZnO nanowires and quasi-spherical Ag crystals. ZnO NWs exhibited hexagonal wurtzite

structure and cubic FCC symmetry in Ag nanoparticles (NPS). Two types of nanostructures, including homogeneous cylindrical ZnO NWs in the absence of Ag and simultaneous presence of ZnO NWs and Ag NPs, formed depending on experimental conditions. The photocatalytic activity was evaluated by studying methylene blue (MB) degradation time under UV light excitation. Diffuse reflectance UV–Vis spectrophotometry (UV–Vis DRS) allowed identifying the ZnO absorption band at ~393 nm. Crystal size varied depending on the reaction time and the addition of CTAB. Synthesis time increased bandgap values, getting better photocatalytic performance in samples synthesized in intermediate times (6 h), higher Ag+/Zn2+ molar ratio (0.2/1.0), and CTAB. According to HRTEM observations, the presence of silver nanocrystals with high content of defects (twinning, stacking faults) could play an essential role in the photocatalytic response. In this context, the specific synthesis conditions of Ag/ZnO might be more appropriate for their use in organic dyes degradation in water and the potential use in protective treatments against materials biodeterioration processes.

1-9 Aim of the Study

In order to investigate the reaction behavior of synthesis of ZnO nanoparticles as optical and photocatalytic systems, this study has been set to achieve the following:

1. Preparation of pure ZnO nanoparticles by Solvothermal method.
2. Preparation of Ag/ZnO nanoparticles by photodeposition.

3. Investigation the charectrazation of nanocomposite using different instrument such as XRD.
4. Using SEM and TEM techniques to investigation of structural, surface , morphology and optical properties .
5. Studying photocatalytic activity under different conditions such as the concentration of the Nano-compound, catalyst concentration of pollutants and light intensity.
6. Role of doping Ag on the surface of ZnO to enhance the activities of binary nanocomposites in the photocatalytic degradation of brilliant green dye .

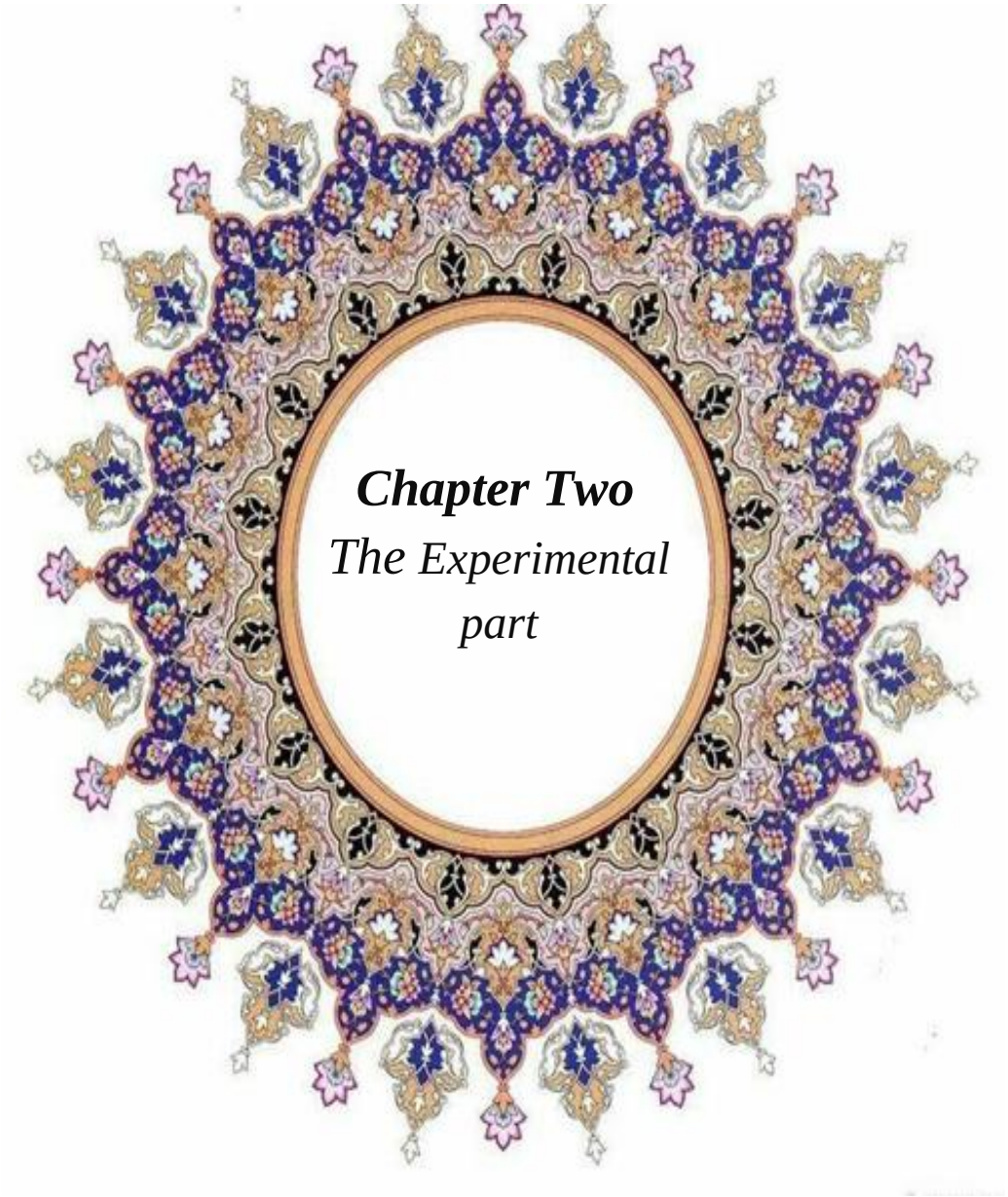

Chapter Two

The Experimental part

2-1 Chemicals

The Chemicals used in this work are listed in table (2-1). All Chemicals were used without further purification.

Table (2-1): Chemicals for all Component

No.	Chemicals	Formula	Manufacturer	Purity%
1	Zinc acetate	$Zn(CH_3COO)_2 .2H_2O$	Sigma-Aldrich	99.999
2	Oxalic acid	$H_2C_2O_4$	India Production	99.8
3	Silver nitrate	$AgNO_3$	Sigma-Aldrich	99
4	Methanol	CH_3OH	Scharlau	99.5
5	Brilliant green	$C_{27}H_{33}N_2.HO_4S$	Sigma-Aldrich	99.5

2-2 Instruments and Equipment

The instruments used in this study with their company are listed in table (2-2) .

Table (2-2): The list of Instruments was used in this project.

No.	Instrument	Manufacturer	Location	Using
1	UV-Visible spectrophotometer	UV-Vis-1650PC Shimadzu , Japan	college of science for Women-Babylon University	UV-VIS spectroscopy

2	X-Ray Diffraction	Siemens – D 5005/ Germany	University of Tehran	stress measurements as well as for texture analysis
3	FE-SEM	TESCAN ,Czechia Republic.	University of Tehran	examine smaller-area spots at electron
4	Oven	Oven Bs Size Two Gallenkamp / England	college of science for Women-Babylon University	material drying
5	Furnace	Muffle Furnace Size Two Gallenkamp / South of Korea	college of science for Women-Babylon University	burning material
6	Centrifuge	Z 200A Hermle/ Germany	college of science for Women-Babylon University	material separation
7	Rotary Evaportion	Bergh of/Germany	college of science for Women-Babylon University	especially for separation purposes
8	Ultrasonic cleaner (power sonic 420)	China	college of science for Women-Babylon University	Helps to hold the material
9	Transmission Electron Microscopy (TEM)	912AB model, Leo, Germany	University of Tehran	Provide morphologic, composition and crystallographic information
10	Band gap energy measurements	UV/ Visible Shimadzue 2700	college of science for Women-Babylon University	Finding the energy gap
11	LED/ UVA specific wavelength 365 nm	USA/Thor lab company	college of science for Women-Babylon University	lowest peak irradiance

2-3 Preparation of Nanomateriales

2-3-1 Preparation of Zinc Oxide Nanoparticles

The solvothermal method was used to prepare ZnO nanoparticles . Firstly, in a beaker dissolve 5 gm of zinc acetate in 150 ml of distilled water, in another beaker dissolve 8 gm of Oxalic acid in 150 ml of distilled water.

Then mix the two chemical compounds above and the series of chemical reactions that takes place. The complete hydrolysis of zinc acetate with the Oxalic acid $H_2C_2O_4$ of in water should result in the formation of a ZnO colloid. The resulting solution was transfer into the rotary (flask) , Afterward the (Rotary flask) was contact with the sealing ring made of (Teflon + Viton) materials of the rotary evaporation device as shown in **Figure (2-1).** Then we turn on the device and regulate the temperature of the heater (stainless water bath) at different temperatures (30-50°C) and the water cooling temperature (refrigerant) at (15°C), and finally the mixture is dried inside the flask under vacume pressure.

The final product was obtained as a result of the equilibrium between hydrolysis and the condensation reaction. Due to heating, zinc acetate inside the solution undergoes hydrolysis forming acetate ions and zinc ions. The overall chemical reaction to form ZnO Nano powder is as follows in equation:

$$\mathbf{Zn(CH_3}\boldsymbol{COO}\mathbf{)_2.2H_2O} + \mathbf{H_2}\boldsymbol{C_2O_4} \rightarrow \boldsymbol{2CH_3COOH} + \boldsymbol{ZnO} + \boldsymbol{2CO_2} + \boldsymbol{2H_2O} \quad \textbf{(2-1)}$$

The resulting residues are washed several times with distilled water until pH is equal to 7 and placed for drying in the oven at a temperature of about 60°C overnight, then ground in a mortar and turned into a fine powder. The obtained white powder is subjected to calcination at (500°C) for one hour.

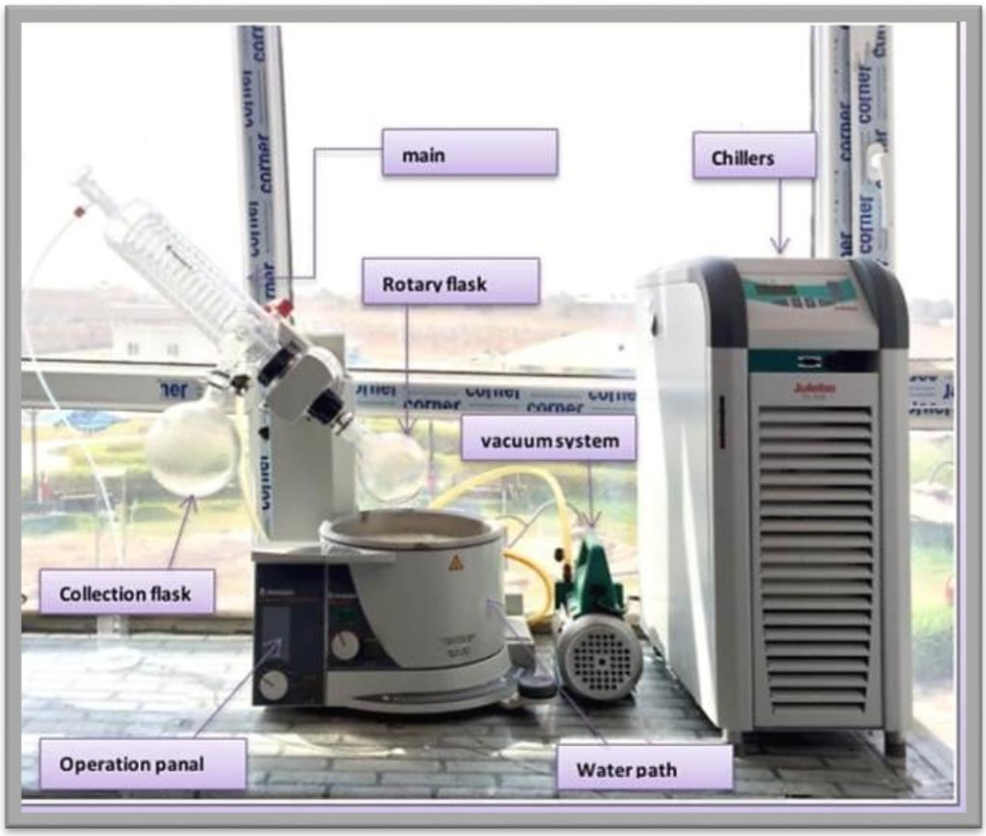

Figure (2-1): The Rotary Evaporation Device, College of Science for Women- University of Babylon.

The main components of a rotary evaporator are:

1) A motor unit that rotates the evaporation flask or vial containing the user's sample.
2) A vapor duct that is the axis for sample rotation, and is a vacuum-tight conduit for the vapor being drawn off the sample.
3) A vacuum system, to substantially reduce the pressure within the evaporator system.
4) A heated fluid bath (generally water) to heat the sample.
5) A condenser with either a coil passing coolant, or a cold finger into which coolant mixtures such as dry ice and acetone are placed.
6) A condensate-collecting flask at the bottom of the condenser, to catch the distilling solvent after it re-condenses.
7) A mechanical or motorized mechanism to quickly lift the evaporation flask from the heating bath.
8) Chillers for cooling water in condenser.

2-3-2 Preparation of Metal Doped ZnO Nanocomposites

Metal doped ZnO was prepared by suspending (1) gm of ZnO powder in (100) ml of distilled water and (3) ml of $AgNO_3$ (0.01) M by sonication for 3 mints, followed by exposing the surface of the mixture to nitrogen gas for 10 mints under continuous magnetic stirring . Then (1 ml of methanol) was added, after which the mixture was irradiated with light intensity (1.71) $mW.cm^{-2}$ (using UVA LED lamp) overnight as shown in **Figure (2-2)** . After

irradiation, the resulting powder was washed with distilled water several times and dried overnight in an oven at 60°C. The same previous work steps are repeated by taking 2 ml of $AgNo_3$ 0.5 ml of methanol . We take 2 ml of $AgNo_3$ 1 ml of methanol .

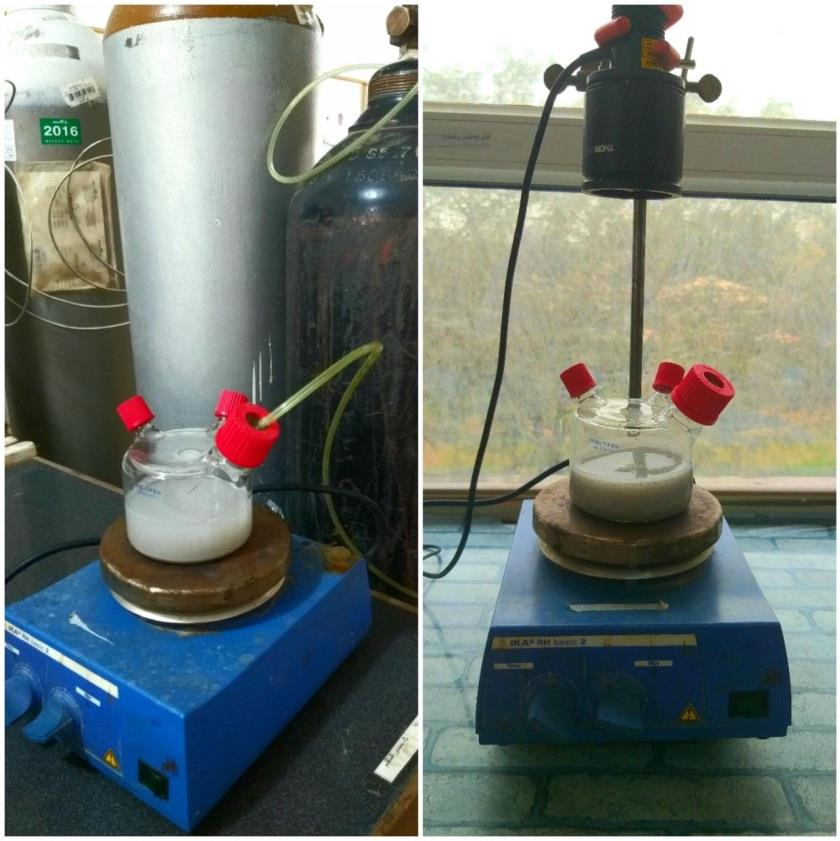

Figure (2-2): Real image for the photodeposition of silver doped ZnO (a) pugulate the mixed surface to nitrogen gas (b) Irradiate the mixture with a lamp LED

2-4 Characterization Techniques

Different techniques were used to characterize and study the structure and nature of nanomaterial . Thus, the common techniques were explained briefly in the following :

2-4-1 X-Ray Diffraction (XRD)

X-ray diffraction is a powerful non-destructive technique for characterizing crystalline materials. It provides information on the preferred structures, phases, and orientations (texture) of crystals and other structural parameters, such as average grain size, crystallinity, strain, and defects of crystals[65].

The determination of crystal or grain size is based on the principle that a decrease in crystal size leads to an increase in diffraction width (peak broadening). Hence, an increase in width is an indication that there are not enough levels in the small crystals to produce a complete destructive interference.

In 1918 Debbie Shearer formulated an equation for the estimation of particle size as follows :

$$D = \frac{k\lambda}{B\cos\theta} \qquad (2\text{-}3)$$

where, D = particle size, θ = angle of diffraction, K= Scherer constant (=0.9), λ= x-ray wavelength, B = full wide that half maximum (FWHM) that is measured in radian [66].

X-ray diffraction measurement had been done according to the **SIEMENS – D5005 X-ray** diffractometer Figure. (2-3) of wavelength 1.54433 A°, the dried powder prepared using the method in section (2-3) at different preparation conditions.

Figure (2-3): A photo of XRD device , University of Cranfield – United Kingdom.

It is important to note that the Scherer equation can only be used for average sizes of up to about 100 nm. It also depends on the instrument, as well as the relationship between the signal and the sample with standard noise, because the larger the crystal, the lower the diffraction peak amplitude. It can be very difficult to provide separation and distinction between expansion by crystal size and expansion due to other factors and factors. Errors are always present and successful calculation methods are

those that can reduce errors in the best possible way to obtain more accurate data[67].

2-4-2 Field Emission Scanning Electron Microscopy (FE-SEM)

The field emission scanning electron microscopy is an ideal analytical technique for characterizing and visualizing the elemental composition of a specimen[68] . It has a spatial resolution of <1 nm and a number of other advantages, including much improved performance at low accelerating voltages[69] . It has recently becomes more popular because high magnification image can be taken under high vacuum condition. This technique is widely used in metals, semiconductors, ceramics, medical and biological field [70] .

The properties of FE-SEM allow the emergence of new approaches to life science studies, based on high quality, low-voltage images with negligible electric charge of the samples, producing clearer images with less electrostatic distortion with a spatial resolution of 1.5 nm which is 3 to 6 times better than traditional SEM. The low penetration of the low kinetic energy electron probes closest to the immediate material surface can be examined, and the smaller contamination areas can be examined at electron accelerating voltages compatible with energy dispersive X-ray spectroscopy [71].

The ultra-high resolution of FE-SEM offers new insights into the dynamical processes of interactions between nanoparticles and cells Figure (2-3). FE-SEM images of the ZnO powder were taken by using **FEI model XL 30 (formally Philips).**

Figure (2-4): A Photo of FE-SEM Microscope, University of Canfield - United Kingdom

2-4-3 Transmission Electron Microscopy (TEM)

TEM is a technique developed to get magnification and hence details of a specimen to much improved level that the conventional optical microscopes . TEM produces numerous information of materials at including size distribution . morphology , crystal structure, TEM can be used in various application such as research, science of nanotechnology and educational . The TEM is based on the theory where abeam of electrons are imposed on the surface of the specimen nanoparticles , they can scatter or backscatter elastically or in elastically or produce many interactions . TEM is the powerful magnified of TEM microscope reach to 1nm particle that can

be also calculated .The TEM produce a 2D images with high resolution capacity[72].

2-4-4 Ultraviolet-Visible Spectroscopy(UV-Vis)

Ultraviolet-Visible spectroscopy is a method refers to absorption or reflectance spectroscopy through the regions of ultra violet and visible spectrum UV-Vis spectrum can be measured as an absorption / transmission spectrum . the wavelength range of UV from (100-400) nm can be consider shorter than the visible light (400-800) nm . It can be measures the intensity of light passing through the sample[73].

2-4-5 Band Gap Energy Measurements

A semiconductor is a material that has low electrical conductivity at room temperature, but its conductivity increased by input of energy. The solid material composed of an inconceivable number of atoms and contains an infinite number of energy states. Because these energy levels are so closely spaced, they form bands instead of discrete energy states. This is the major difference between a solid material and a single molecule that contains a finite number of atoms and possesses discrete energy levels. The highest energy band that is filled with electrons is called the valence band. The next higher band that is empty is called the conduction band. The energy separation between these bands is called the band gap, Eg [74] . A Varian Cary 100 Scan UV−visible spectrophotometer system equipped with a lab sphere diffuse reflectance accessory was used to obtain the reflectance spectra as shown in Figure (2-5) Shimadzo Corporation (JAPAN) was employed as a reflectance standard. the bandgap was obtained for ZnO powder.

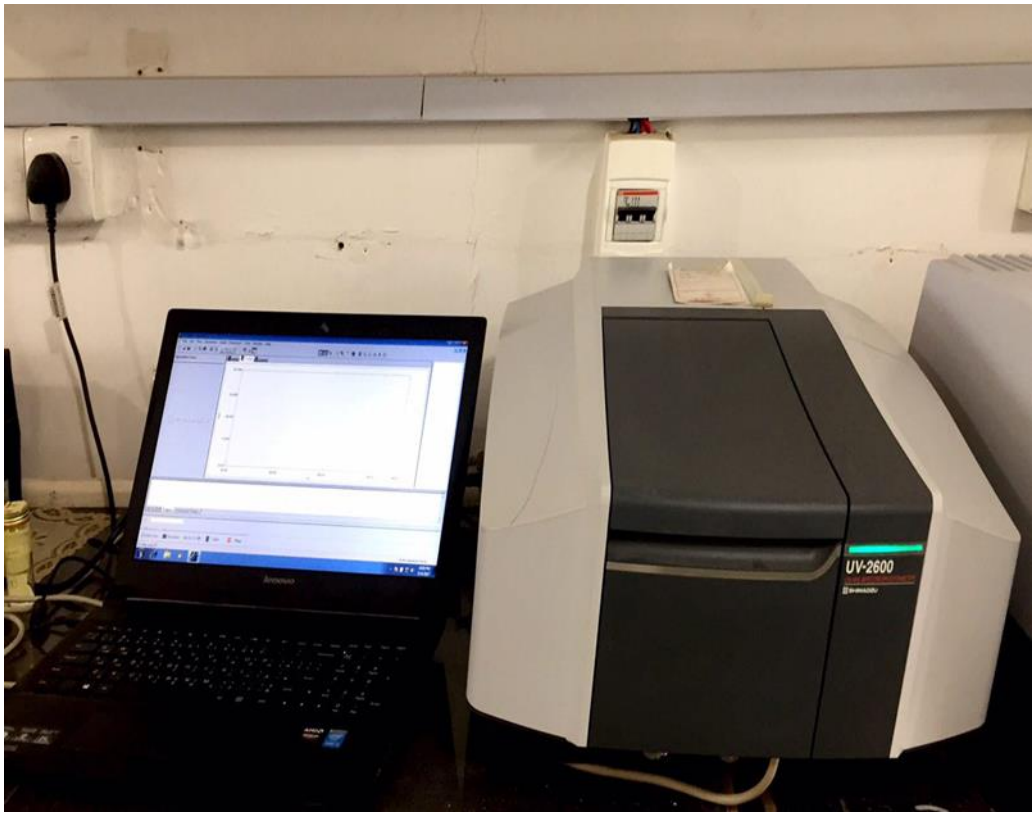

Figure (2-5): A real photo of UV Spectrophotometer Device College of Science for Women / University of Babylon

2-5 Applications of Prepared Nanomaterials

2-5-1 Determination of Maximum Wavelength (λ max) and calibration curve of Brilliant green dye

A standard solution of brilliant green at 100 ppm was prepared by dissolving a specific weight of (0.01gm) brilliant green solid dye in 100 ml of distilled water with stirring to complete the dissolving and then complete the volume. The wavelength of brilliant green dye was taken in the range (200-800) nm using quartz cuvette. The maximum wavelength of the dye

solution was determined from its highest absorption in the UV-Visible spectrum, which was found at the wavelength (λmax= 630nm), the structure of brilliant green dye is shown in Figure (2-6). To construct the calibration curve for the brilliant green dye, a series of solutions were prepared by successive dilution of the dye standard solution and with concentration in the range (5-30)ppm. the absorption of this solution was recorded at (λmax= 630nm). The calibration curve was determined by drawing the relationship between absorbance and concentration as shown in Figure (2-7).

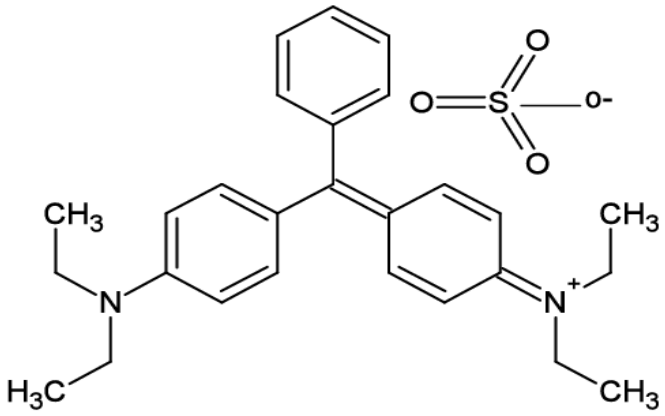

Figure (2-6): Structure of Brilliant green dye

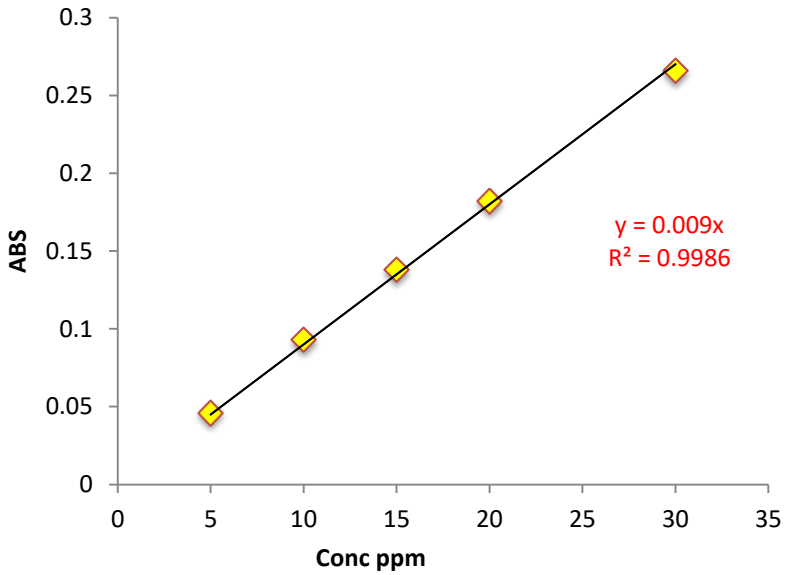

Figure (2-7): Calibration Curve of Brilliant green Dye Solution

2-5-2 Study Effect the Time on the Photodegradation

The effect of time on the photodegradation of the brilliant green dye was studied at different concentrations (10,50,60, 80) ppm /200 ml of the dye solution and is added (0.4)gm of Ag\ZnO to the prepared mixture . Before adding the catalyst to the solution 5 ml of the mixture is taken. After placing the prepared mixture in an ultrasonic cleaner (Power Sonic 420) for the purpose of distributing the catalyst in the dye. The period was recorded under UV light for 90 mints. 5 ml of samples were taken every 15 mints and centrifuged for 30 mints at 3500 rpm to remove the nanostructure of the catalyst. brilliant green pigment absorbency was determined to select the best catalyst weight.

2-5-3 The Suitable catalyst for photodegradation

To determine the best catalyst from all nanomaterials prepared using the following assay: We tested each catalyst separately by taking (0.2) g of (ZnO, dark gray ($ZnO_{Ag(0.7\%)}$) , light gray ($ZnO_{Ag(0.3\%)}$) , very light gray($ZnO_{Ag(0.2\%)}$) added to 100 ml of Brilliant Green Concentrate 37.5ppm. Before adding the catalyst to the solution, 5 ml of the mixture is taken. After placing the prepared mixture in an ultrasonic cleaner (Power Sonic 420) for the purpose of distributing the catalyst in the dye. The period was recorded under UV light for 1 hour. The withdrawn samples were placed in a centrifuge at 3500 rpm, using a UV spectrometer (1650), Shimadzu, and the absorption contrast was monitored at (630 nm). The absorbance of the withdrawn samples was recorded.

2-5-4 Study the concentration Effect of Brilliant green dye

The effect of the bright green dye under ultraviolet light at variable concentrations of 20-50 ppm in the presence of 0.2 g of (Ag-ZnO) was on the photolysis efficiency of the catalyst. The absorption was recorded after irradiation under UV light for 1 hour and the best concentration of brilliant green dye was obtained**.**

2-5-5 Effect light intensity

The effect of light intensity on the photolysis of Brilliant green dye at a concentration of 20 ppm under ultraviolet light of variable intensity (1.05, 1.71, 2.97, 5.12) $mW.cm^{-2}$ in the presence of 0.2 g from (Ag-ZnO) on the photolysis efficiency of the catalyst was studied. Before adding the catalyst to the solution 5ml of the mixture is taken . After placing the prepared

mixture in an ultrasonic cleaner (power sonic 420), for the purpose of distributing the catalyst in the dye .The irradiation period was recorded under UV light for 1 hour. After centrifugation at 3500 rpm, using a UV spectrometer (1650), Shimadzu, and observing the absorption contrast at (630 nm). The absorbance of the drawn samples was recorded.

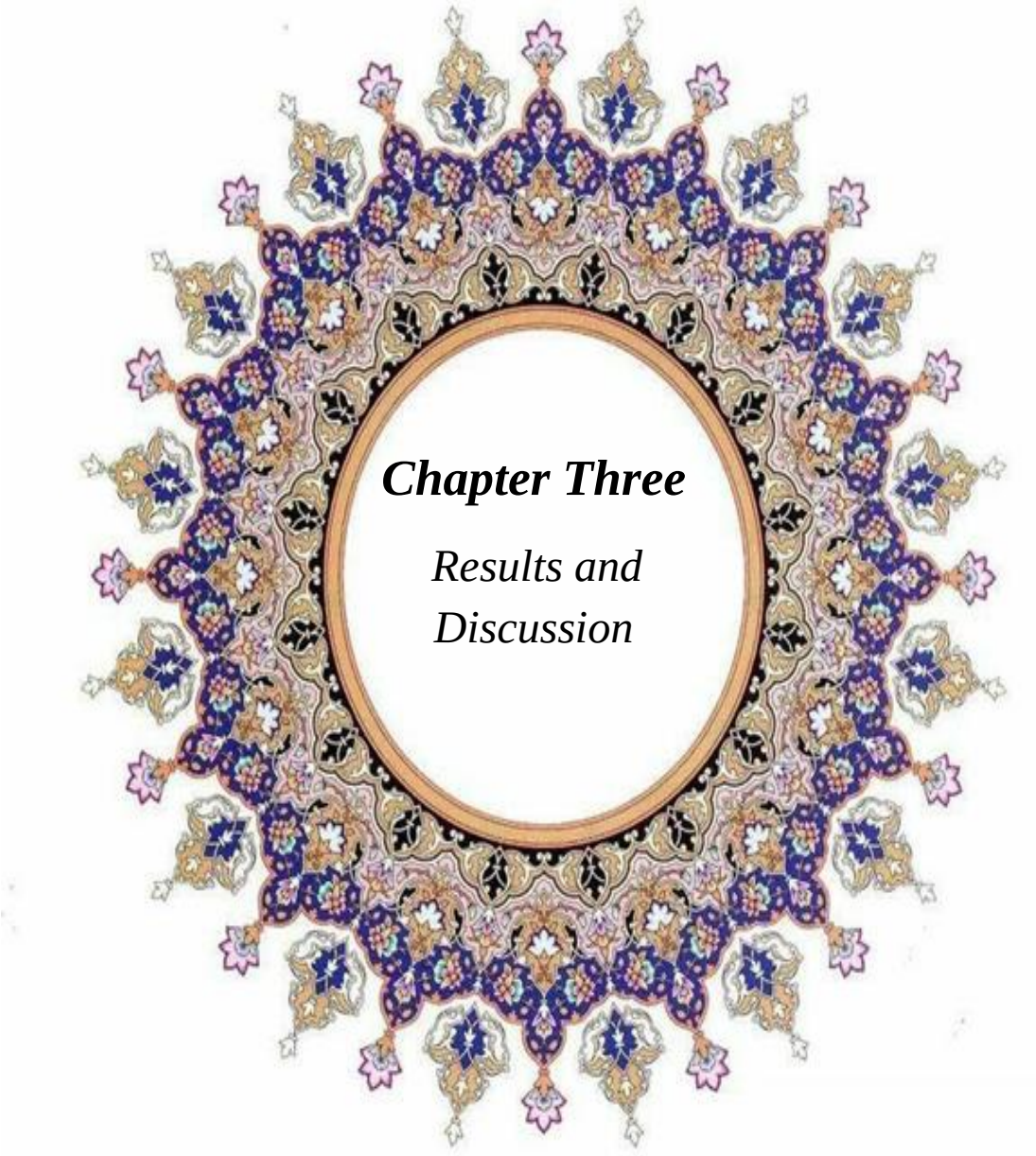

Chapter Three

Results and Discussion

3-1Characterization of Zinc Oxide and Silver Nanocomposite

3-1-1 XRD diffraction of ZnO and Ag-ZnO nanocomposite

In **Figure.3-1** show the XRD patterns at of prepared ZnO and Ag-ZnO . In **Figure.3-1 (a)** the XRD pattern of ZnO there are no other summit indicate the presence of the impurity, this is indication that these nanoparticles of zinc oxide possess one phase. The impurity patterns observed due to effect of calcination .Nine peaks appear at 31.7°, 34.4°, 36.2°, 47.5°, 56.5°,62.82°, 66.4°,67.9°and 69.10, which correspond to the (100), (002), (101), (102), (110), (103), (200), (112) and (201),reflection planes, respectively. All the diffraction peaks can also be well indicate to the hexagonal Wurtzite structure of ZnO JCPDS card (no. 36-1451) [75, 76] and pure phase with highly crystalline produced due to very sharp and intense peaks[77] .

In Figure. 3-1(b) no crystalline phase involving Ag could be observed. This indicates that the Ag is too dispersed in the ZnO lattice is not sufficient for clear crystal formation or the Ag content is below the detection limit. Interestingly, no Ag crystal phase was detected. Thus, at low Ag content, higher dispersion of smaller Ag nanoparticles is on the surface and pores are clearly achieved.

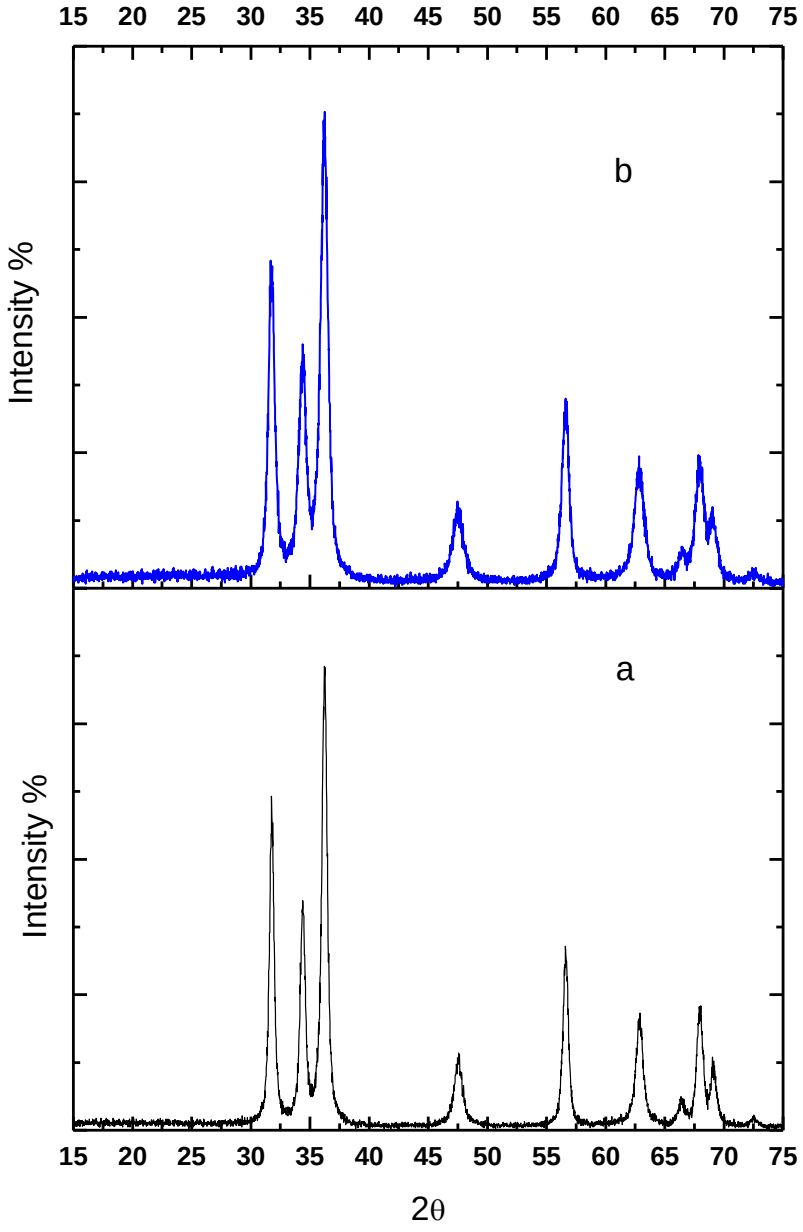

Figure (3-1): XRD Diffraction Patterns of (a)

ZnO Nanoparticles and (b) ZnO $_{Ag(\ 0.2\%)}$) Nanocomposite

3-1-2 SEM of ZnO and Ag-ZnO Nanocomposite

The surface morphology of pure ZnO nanoparticles has been studied in terms of the size, shape of particles and clusters among them, in addition to the distribution of these particles using the SEM technique . Figure . 3-2 (a) shows SEM image of ZnO, the nanoparticles have a hexagonal wurtize shape with a mean size of between (32-60) nm with highly of agglomerate . The SEM image of ZnO $_{Ag(\ 0.7\%,0.3\%\ and\ 0.2\%)}$ respectively in Figure. 3-2 (b, c ,d) shows different types of nanoparticles hexagonal wurtize like morphology for ZnO and Ag nanoparticles with much agglomeration . The morphology is found to be changed in their different percentage, it is observed that there is a difference in the nature and characteristics of the surface of the prepared nanocomposites . Also it can be notice when the concentration of increase the shape of nanocomposites change , the nature of surface is porous and is rough due to the increase of silver nanocomposites on the surface of the size oxide nanocomposites .

Silver nanocomposites were found to be overlapped with ZnO nanocomposites which exhibits cubic like morphology and their particle size ranges from around (37-59) nm for ZnO $_{Ag(0.7\%)}$, also around (53-64) nm for ZnO $_{Ag(0.3\ \%)}$ and around (57-70) nm for ZnO $_{Ag(0.2\ \%)}$ nanocomposites

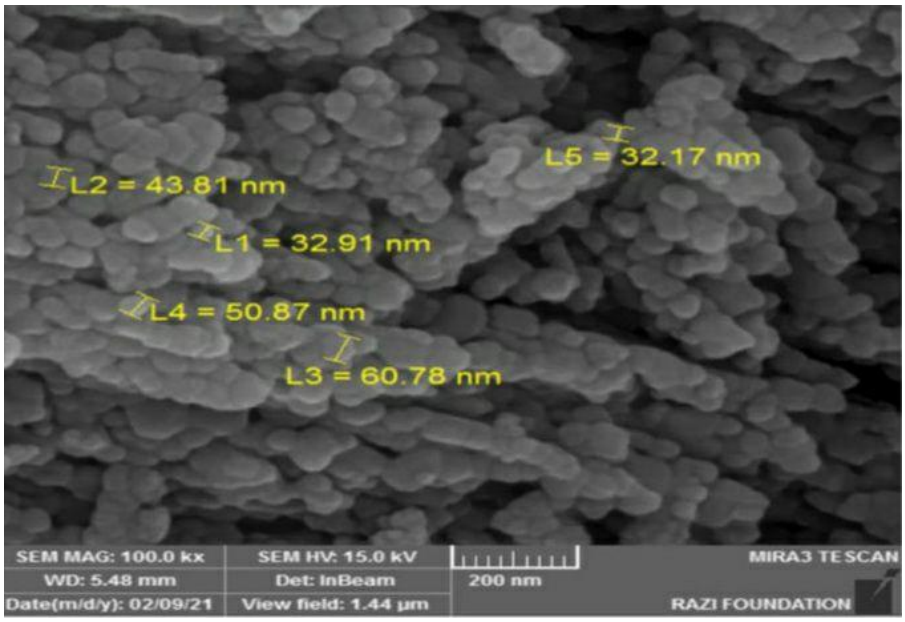

Figure(3-2a): FE-SEM Images of ZnO

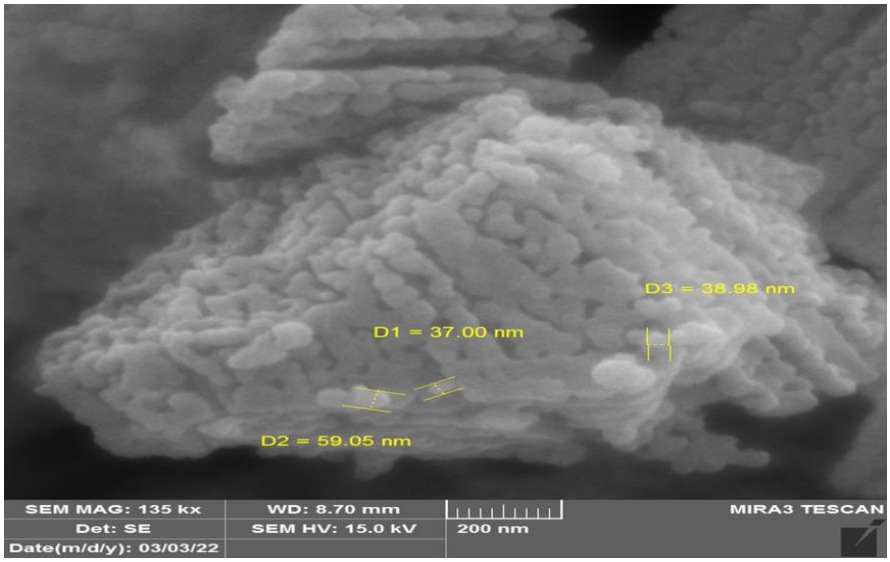

Figure(3-2b): FE-SEM Images of ZnO $_{Ag(0.7\%)}$

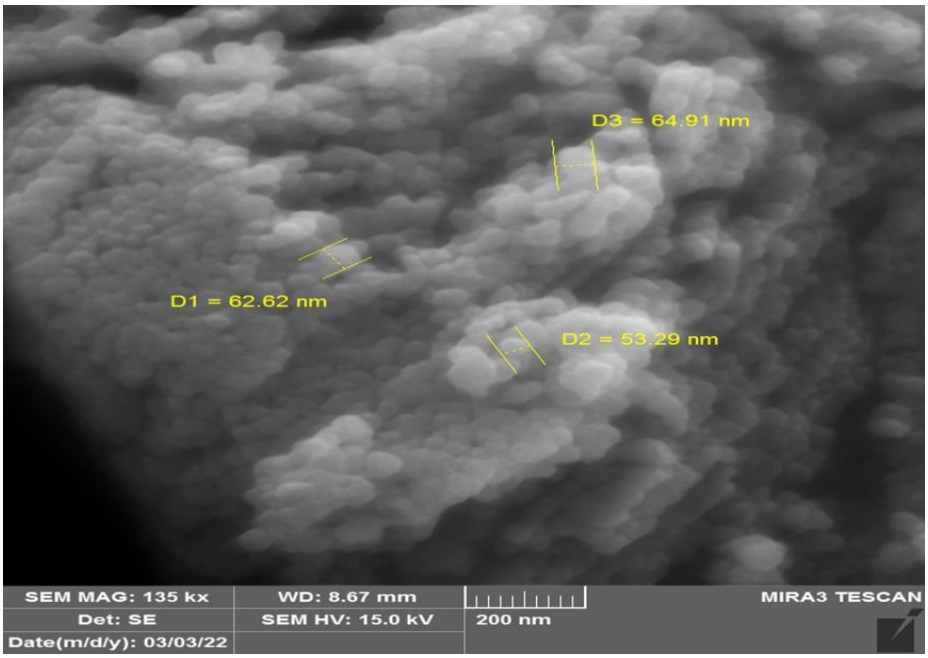

Figure(3-2c): FE-SEM Images of ZnO Ag(0.3 %)

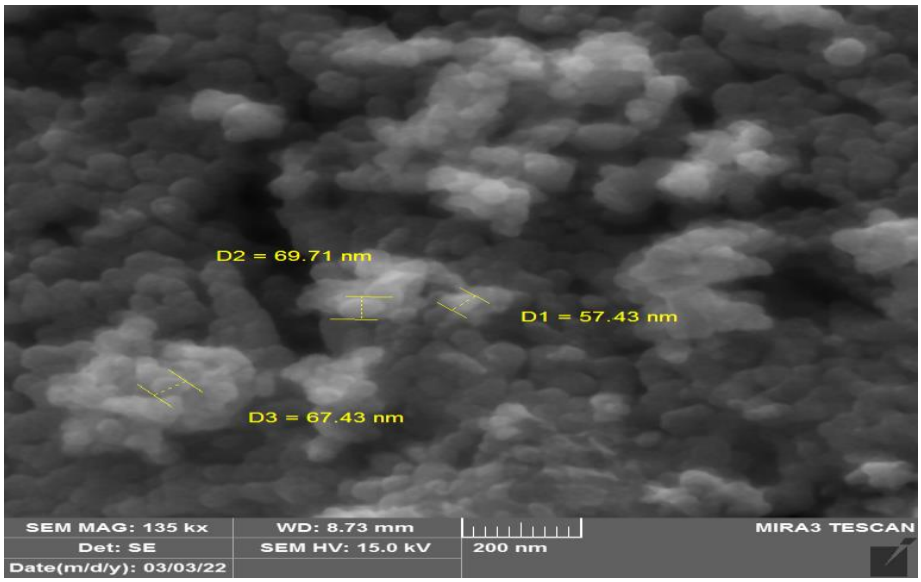

Figure(3-2d): FE-SEM Images of ZnO Ag(0.2 %)

3-1-3 TEM of Ag\ ZnO Nanocomposite

The transmission electron microscopy gives a more accurate picture of the structure of prepared samples ; the crystalline, distribution and the particles size of nanocomposites is shown in Figure.3-3(a , c) The TEM image shows two types of Ag\ ZnO nanoparticles. ZnO nanoparticles appear to be much larger and more agglomerated than Ag nanoparticles. The particle size is approximately equal to (35-80)nm and is spherical-like. Figure .3-3(b)shows that the aggregate of atoms in the nanoparticles is in the form of a polycrystalline. The aggregate TEM image that owing to occur the sintering of silver and zinc oxide crystals which is formed through the photo deposition.

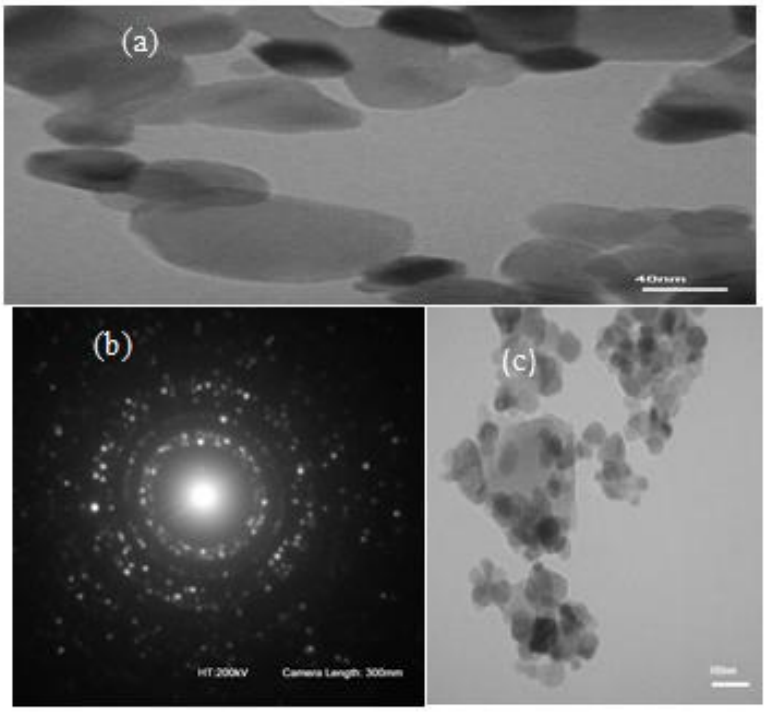

Figure(3-3): (a) and (c) TEM image of Ag\ ZnO nanocomposite, (b) selected area electron diffraction(SAED)of Ag\ ZnO

3-1- 4 UV-Vis Spectroscopy of ZnO $_{Ag(0.2\%)}$ nanocomposites

The quantity of the energy band gap of prepared nanocomposites has been determined by studies of optical properties of these particles using UV-Vis

Spectroscopy in the range of wavelengths 300-700 nm .The band gap energy was calculated based on the absorption spectrum of the sample according to the following equation :

$$E_{bg} = 1240/\lambda g \qquad (3\text{-}1)$$

Where, E_{bg} is The band gap energy of the photo catalytic, λg is the wavelength in nm used the absorption edge. Also the band gap of nanocomposites can be calculated by Tauc's plot which is expressed as follows

$$(\alpha h\nu)^{1/n} = Cx\ (h\nu - E_{bg}) \qquad (3\text{-}2)$$

Where α is the absorption coefficient, h is Planck's constant, ν is frequency ($\nu = c/\lambda$, c light speed, λ is the wavelength). n = ½, 2 for direct and indirect

band gap, respectively[78]. C is proportionality constant, and E_{bg} is band gap. The results for pure ZnO in Fig shows blue shifted and no absorption in visible range with strong UV absorption at 370 nm, the calculated band gap of ZnO nanoparticles was found to be 3.32 Ev , this indicates that the ZnO is related to the Wurtzite structure of ZnO crystal and may be due to change transfer band from O:2p to Zn:4s[79, 80] .

In metal nanoparticles such as in silver, conduction band and valence band lie very close to each other in which electrons move freely . These free electron give rise to surface Plasmon resonance (SPR) absorption band ,occurring due to the collective oscillation of electrons of silver nanoparticles in resonance with light wave . Classically, the electric field of an incoming wave induces polarization of the electrons with respect to much heavier ionic core of silver nanoparticles. As a result a net charge difference occurs which in turn acts as a restoring force .This creates a dipolar oscillation of all the absorption edge shifted to red shift and the band gap energy decreases indicating to the silver doped with ZnO nanoparticles[81, 82] . The ZnO $_{Ag(0.2\%)}$ in Figure (3-4) has low absorption in visible region .

This improvement in the optical absorption of ZnO by the increase of defect sites on the catalyst structure which can inhibit the recombination of the charge carriers and improve the photocatalytic activity of ZnO . According to the results, the band gap slowly decreases with the increase of the Ag doping ZnO and small change was observed[83, 84] .

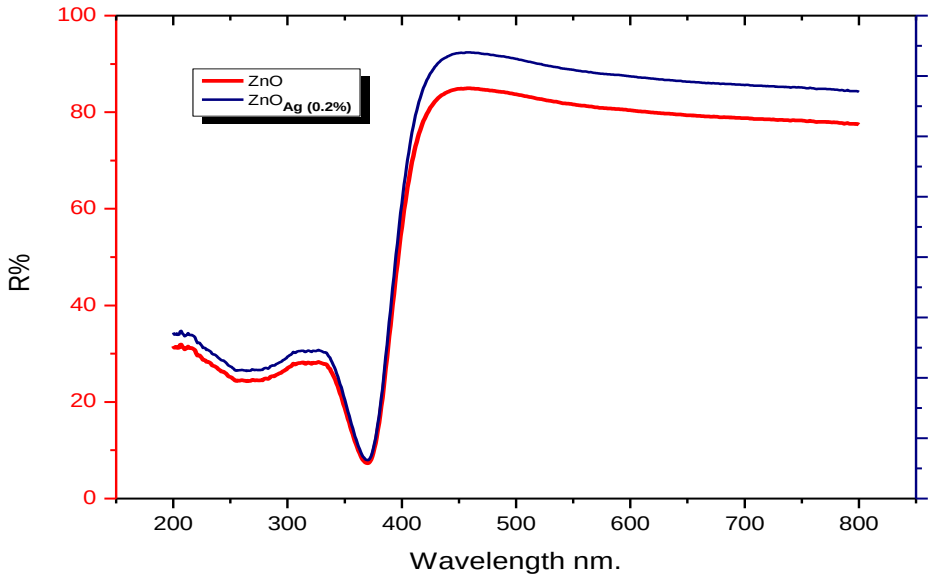

Figure (3-4): Diffuse Spectra of ZnO Nanoparticles and ZnO $_{Ag\ (0.2\%)}$ Nanocomposites

3-2 Application of Prepared Nanocomposites

3-2-1 Selectivity of the Best Photo Catalyst Surface

The Ag content plays an important role in increasing the optical efficiency and preventing electron-hole pair recombination. It is known that noble metal nanoparticles deposited on the surface of ZnO act as effective traps for photogenerated electrons due to the formation of a Schotkky barrier upon contact with metallic semiconductors. These electrons improve the rate of oxygen reduction and prevent electron-hole recombination[85].

Under illumination, when ZnO and Ag nanoparticles come into contact, the photogenerated electrons are distributed between both types of particles,

resulting in electron transfer from excited ZnO to Ag , until the two systems achieve equilibrium. The electron accumulation of the Ag particles increases the Fermi level to more negative potential, which also causes a shift in the Fermi level of the compound closer to the conduction band of the composite[80].

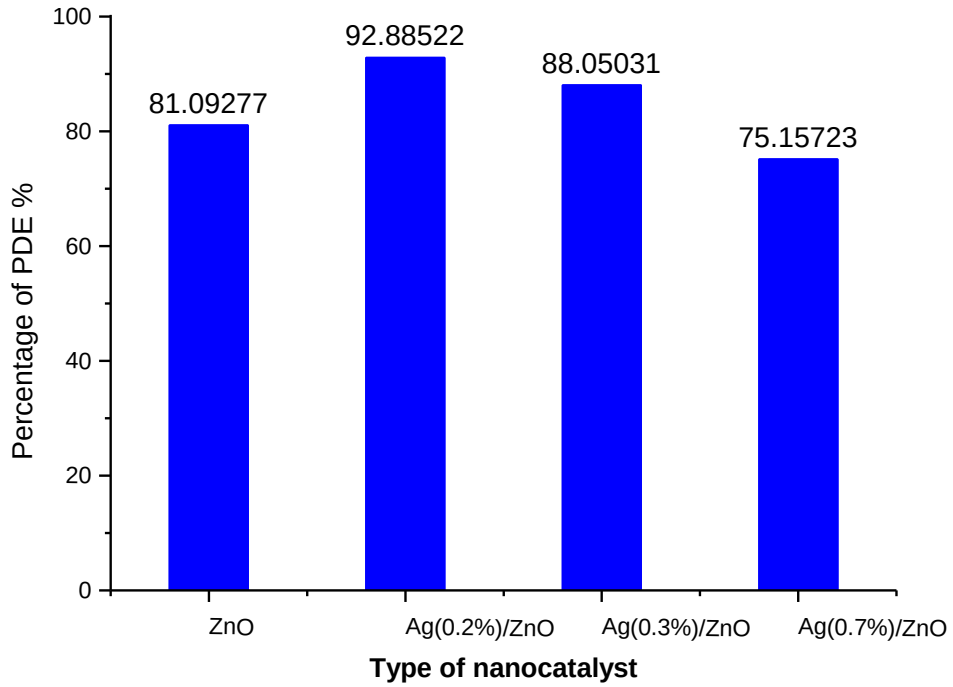

Figure (3-5): Selectivity of the best photo catalyst surface P.D.E. % with type of Nano catalyst

Figure(3-5) shows a significant and noticeable increase in the photocatalytic degradation efficiency of ZnO $_{Ag(0.7\%)}$. In contrast, a decrease in the photolysis efficiency of the remaining types of nanocatalysts. A

similar dependence of photolysis efficiency on the amount of Ag loading has been documented previously[86].

The photolysis efficiency of Ag/ZnO undergoes the smaller the amount of Ag on the ZnO surface. Because of the less agglomeration of some small particles, the dispersion of Ag usually decreases with the increase in the amount of load. Decreased quantity results in low efficiency of Ag and weak photoactivity of Ag/ZnO. In addition to Ag scattering, the photocatalytic degradation efficiency of Ag/ZnO is also affected by Schotkky barriers between the surface of Ag and ZnO[40].

When the Ag content is in the right amount, the number of Schotkky barriers at the Ag/ZnO interface is enhanced by increasing Ag loading, which leads to an increase in the photocatalytic degradation efficiency[87].

However, when the Ag loading is less than the amount as in type Ag1\ZnO, the active sites on the ZnO surface that are available for light absorbers and electron donors are covered with excess Ag particles. Moreover, some Ag particles may act as recombination centers for photogenerated electrons and holes [41].

3-2-2 Concentration Effect of Dye

In order to evaluate the application of the solution grown Ag/ZnO nanocomposite as a catalyst for the photodegradation of the textile pollutant brilliant green dye. The initial concentration of dye solution plays a pivotal role in deciding the rate of dye degradation. We have carried out

their photocatalytic degradation kinetics at room temperature in presence of the UVA light using a wavelength of 365nm (3.39 eV)[88].

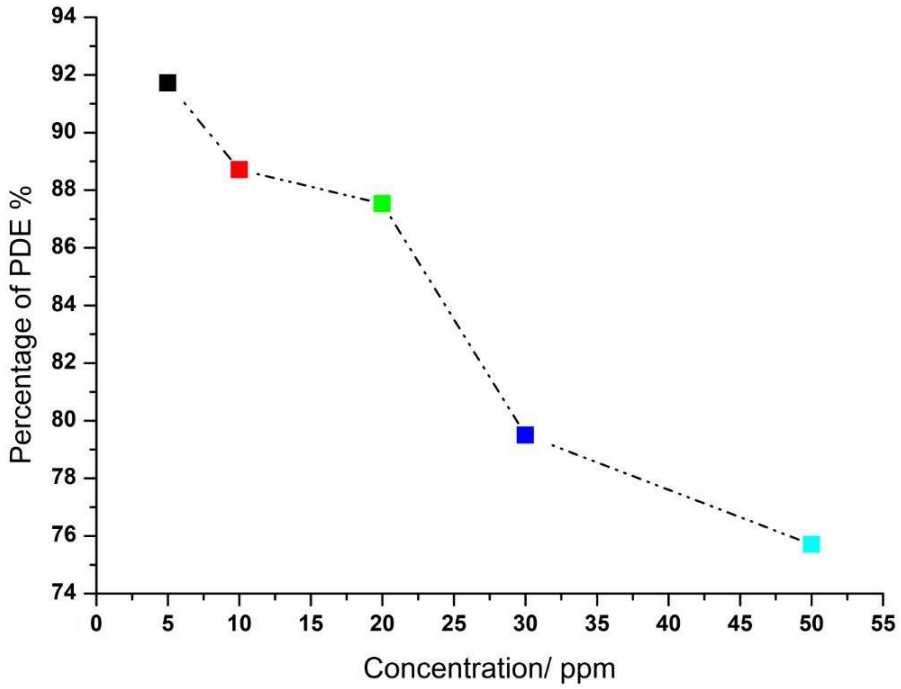

Figure (3-6): Effect of Brilliant Green Dye Concentration P.D.E. % of Ag/ZnO nanocomposite

Figure (3-6) shows that with an increase in the dye concentration, the photocatalytic degradation efficiency increased and reached a maximum at the dye concentration of 5 ppm . Beyond this optimum dye concentration, a further increase in dye concentration led to a decrease in the photocatalytic Degradation Efficiency . At relatively high concentrations of dye beyond the

optimum point, although the surface active sites remain constant for a fixed catalyst concentration, the number of adsorbed dye molecules accommodated on the photocatalyst surface increases[89].

Because the generation of valence band holes on the surface of the photocatalyst required for reacting with dye molecules does not increase as the intensity of light and the amount of catalyst are unchanged, there was an observed decrease in the photocatalytic Degradation Efficiency, probably due to the blockage of the adsorption of hydronium cations at surface active sites, so as to be reduced to produce hydrogen. At a low dye concentration, the rate of photocatalytic reaction is limited by the mass transfer of dye from solution to the Ag/ZnO surface. However, at a middle dye concentration, due to the gradual adsorption saturation of dye on the Ag/ZnO surface, the interfacial reactions govern the overall process. Furthermore, at a high dye concentration, the active sites on the Ag/ZnO surface may be covered by excessive dye adsorption and thus the hydroxyl radicals in dye hydrolysis decrease resulting in a lower dye degradation rate[90].

3-2-3 Light Intensity Effect on Photodegradation of the Dye

Light intensity determines the extent of light absorption by the semiconductor catalyst at a given wavelength. The rate of initiation of photocatalysis, electron hole (e^-/h^+), formation in the photochemical reaction is strongly dependent on the light intensity[91].

Light intensity distribution within the reactor invariably determines the overall pollutant conversion and degradation efficiency. Consequently the dependency of pollutant degradation rate on the light intensity has been studied in numerous investigations of various organic pollutants[92].

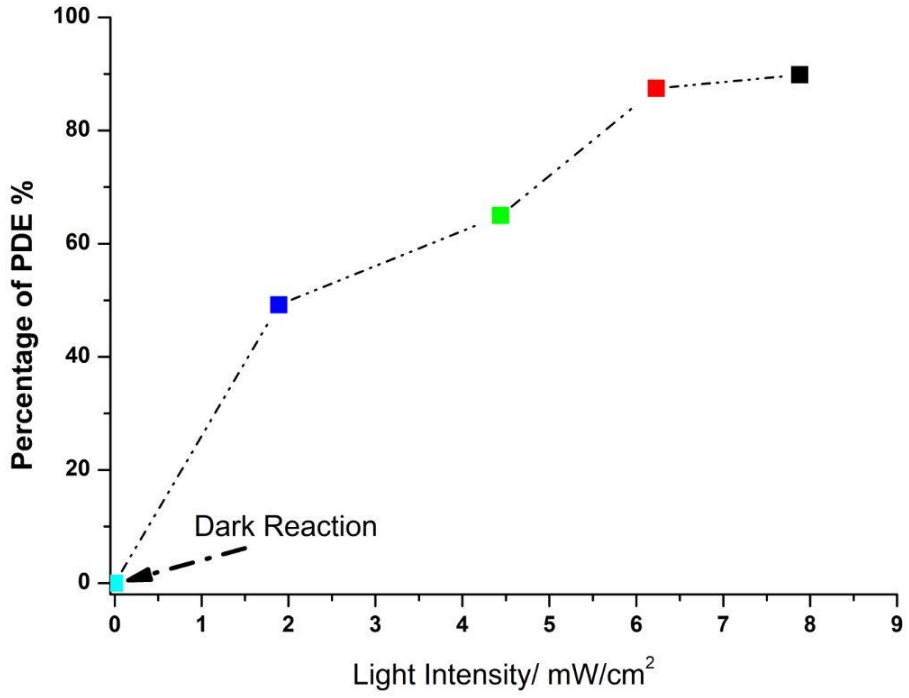

Figure (3-7): Effect of Light Intensity on P.D.E. % of Brilliant Green Dye

Figure (3-7)shows that a linear relationship is observed between light intensity and photocatalytic degradation efficiency. The rate of photocatalytic degradation efficiency increases with the intensity of the UV

light as more radiation falls on the catalyst and therefore more hydroxide radicals[93].

They are produced resulting in a high rate of photocatalytic degradation efficiency.

It has been shown from Figure(3-7). that at low light intensity (0- 4.5 mW. cm^{-2}), the rate will increase linearly with increasing light intensity (first order), while at intermediate light intensity (6.5 mW.$c\bar{m}^{2}$) the rate will depend on the square root of light intensity, in high light, and rate independent of light intensity. Low intensity reactions involving electron-hole formation (e^{-}) is predominant and electron-hole recombination (e^{-}) non-significant[94]. In the lower light intensity range, the higher the incident light intensity led to a greater increase in the absorption potential between photons and active sites on the ZnO surface. On the other hand, when the light intensity increases, the separation between electron and holes competes with recombination, causing the reaction rate to decrease[95, 96].

3-2-4 Role of Time on Photocatalytic Degradation

It is important to initially establish whether the degradation reaction takes place in the adsorbed state (dye adsorbed to ZnO powder) or the ZnO semiconductor surface merely provides an active species (^{-}OH) adsorbed into solution and subsequently reacts. The L-H treatment is known to be a good model for the description of solid-gas reactions. Extrapolation of this model to solid-liquid reactions requires some modifications, especially when the surface is that of ZnO particles in aqueous solutions[97] . The ZnO is known to be covered with hydroxyl groups and molecular water. When is

ZnO illuminated with the light intensity (I) of λ< 390 nm, or with energy greater than the ZnO band gap, an electron is promoted from the valence band and leaves holes (h^+) to the conduction band, which generates electron (e^-) –hole (h^+) pairs (equation 3-3)

$$\mathbf{ZnO + h\nu\ (Ia)} \xrightarrow{K1} \mathbf{e^- + h^+} \qquad \mathbf{(3\text{-}3)}$$

Some electrons and holes combine and produce heat according to equation(3-4):

$$\mathbf{e^- + h^+} \xrightarrow{k2} \mathbf{heat} \qquad \mathbf{(3\text{-}4)}$$

In aqueous medium, at the pHs lower than pH_{pzc} of ZnO, positively charged active sites of ZnO surface (S_{ZnO}) adsorb water molecules and negatively charged hydroxyl ions as in equation(3-5)[98]

$$\mathbf{H_2O + OH^- + ZnO} \xrightarrow{k3} \mathbf{H_2O_{ads} + OH^-_{ads}} \qquad \mathbf{(3\text{-}5)}$$

The holes in the ZnO valence band, having an oxidation potential of +2.6V versus normal hydrogen electrode (NHE) at pH = 7, can oxidize water or hydroxide to produce hydroxyl radicals as in equations
(3-6 and 3-7)[99]

$$h^+ + H_2O_{ads} \xrightarrow{k4} OH^{\cdot}_{ads} + H^+ \quad \textbf{(3-6)}$$

$$h^+ + OH^-_{ads} \xrightarrow{k5} OH^{\cdot}_{ads} \quad \textbf{(3-7)}$$

The active species such as ˙OH radicals could attack the pre-adsorbed organic molecules and inactive species[100] . Equation(3-8a), shows the first step of dye adsorbed on the dye surface, equation(3-8a) represents the photocatalytic degradation of the dye molecules. Besides reaction (3-8), the inactive sites on ZnO surface ($I_{inactive}$) interfere in the process of quenching hydroxyl radicals (equation 3-9). The intermediates of dye degradation react with hydroxyl radicals to complete mineralization (equation 3-10)

$$\textbf{Dye + ZnO} \xrightarrow{K_{ads}} \textbf{dye}_{ads} \quad \textbf{(3-8a)}$$

$$OH^{\cdot}_{ads} + \textbf{dye}_{ads} \xrightarrow{k6} \textbf{Int} \quad \textbf{(3-8b)}$$

$$\textbf{vfbr } OH^{\cdot}_{ads} + \textbf{S inactive} \xrightarrow{k7} \textbf{Inactive species} \quad \textbf{(3-9)}$$

$$OH^{\cdot}_{ads} + \textbf{Int.} \xrightarrow{k8} \textbf{product} \quad \textbf{(3-10)}$$

The hydroxyl radical species can be deactivated by de-trapping of holes or via reaction with surface electrons considering the recombination of ˙OH radicals with surface electrons as the major pathway to explain the interdependence of the reaction rate with photon flow and the concentration of the target compound as presented in equations[101] (3-11 and 3-12).

$$OH^{\cdot}_{ads} \xrightarrow{k9} OH^{-}_{ads} + h^{+} \qquad (3\text{-}11)$$

$$OH^{\cdot}_{ads} + e^{-} \xrightarrow{k10} OH^{-}_{ads} \qquad (3\text{-}12)$$

In the photo degradation of dye by UV radiation in the presence of ZnO, it is postulated that the rate-determining step is the reaction between adsorbed $^{\cdot}OH$ radicals and dye. The rate of disappearance of the dye may be represented by the equation (3-13):

$$r_{dye} = k_6[OH^{\cdot}_{ads}][dye]_{ads} \qquad (3\text{-}13)$$

The concentration of photon-induced holes (h^+) can be obtained by applying steady-state approximation as in equations (3-14a) , (3-14b).

$$\frac{d[h+]}{dt} = k_1 Ia - k_2[h^+]^2 - k_4[h^+][H_2O_{ads}] - k_5[h^+][OH^-_{ads}] \qquad (3\text{-}14a)$$

$$\frac{d[h+]}{dt} = k_1 Ia - k_2[h^+][e-] - k_4[h^+][H_2O_{ads}] - k_5[h^+][OH^-_{ads}] \qquad (3\text{-}14b)$$

$$\frac{d[h+]}{dt} = k_1 Ia - k_2[h^+][e^-] - k_A[h^+] \qquad (3\text{-}15)$$

where $k_A = k_4[H_2O_{ads}] + k_5[OH^-_{ads}]$

showed that at low light intensities, h^+ trapping competes effectively with electron-hole recombination as represented in equation (3-16).

$$k_A[h^+] \gg\gg k_2[h^+][e^-] \quad (3\text{-}16)$$

Therefore equation (3-15) can be simplified to:

$$[h^+] = \frac{k1Ia}{kA} \quad (3\text{-}17)$$

Similarly, if the steady-state approximate is used for the concentration of ˙OH radicals, the following equation can(3-18)[102] be obtained

$$\frac{k1Ia}{kA} = k_A[h^+] - k_6[OH^{\cdot}ads][dye_{ads}] - k_8[OH^{\cdot}_{ads}]$$

$$[Int.] - k_7[OH^{\cdot}_{ads}]\ Sinactive - k_9[OH^{\cdot}_{ads}] - k_{10}[OH^{\cdot}_{ads}][e^-] \quad (3\text{-}18)$$

The second assumption is that *k*r is the total reaction rate constant of degradation of the adsorbed dye molecules as represented in equation

(3-18):

$$Kr\ [dye_{ads}] = k_6[OH^{\cdot}_{ads}][dye_{ads}] + k_8[OH^{\cdot}_{ads}]\ [Int.]$$

$$+k_7[OH^{\cdot}_{ads}]S \text{ inactive} \qquad (3\text{-}18)$$

Considering the assumption that the •OH radicals should be mainly formed from the adsorbed H_2O molecules. As a consequence, the concentration of the $[OH_{ads}]_0$ for a single compound before any significant amount of by-products can be obtained by using equation(3-18) as follows:

$$[OH^{\cdot}_{ads}] = \frac{kA[h+]}{kr[\text{dye ads}]+k9+k10[\bar{e}]} \qquad (3\text{-}19a)$$

$$[OH^{\cdot}_{ads}] = \frac{kA[h+]}{kr[\text{dye ads}]+k9+k10[k1Ia/kA]} \qquad (3\text{-}19b)$$

If we suppose that deactivation of •OH radicals with inactive surfaces (S) is very important than other processes, as represented in equation (3-20):

$$[OH^{\cdot}_{ads}] = \frac{kA}{k7[\text{Sinactive}]}[h+] = kB[h+] \qquad (3\text{-}20)$$

$$kB = \frac{kA}{k7[\text{Sinactive}]}$$

combination of equations (3-17) and(3-20) in equation (3-13) yields:

$$r\text{dye} = kCIa[\text{dye}]ads \qquad (3\text{-}21)$$

$$kc = \frac{kBk1k6}{kA}$$

If the L-H adsorption model is applied to dye in this system:

$$r=kr\theta$$

$$\theta = \frac{\mathbf{Kads[dye]ads}}{\mathbf{1+Kads[dye]ads}} \qquad \textbf{(3-22)}$$

$$r_{\mathbf{dye}}= \frac{kCIaKads[dye]ads}{\mathbf{1+Kads[dye]ads}} \qquad \textbf{(3-23)}$$

Where θ is the fraction of the surface covered by the reactant, the K_{ads} is the adsorption equilibrium constant for dye[103]. suggested that the rate must include competitive adsorption by solvent, intermediates and pollutants. Under these reasonable conditions, equation (3-23) can be written as follows:

$$r_{\mathbf{dye}}= \frac{\mathbf{kCIaKads[dye]ads}}{\mathbf{1+Kads[dye]ads+\Sigma kbCb}} \qquad \textbf{(3-23)}$$

In this equation, K_b is the adsorption equilibrium constant for solvent, intermediates and pollutants [104]made the following assumption:

$$K_{ads}\mathbf{[dye]_0}=K_{ads}\mathbf{[dye]}_{ads}+\sum k_b C_b \qquad \textbf{(3-24)}$$

In this equation $[dye]^0$ is the initial concentration of dye, with substituting equation (3-16)) in equation (3-24) we obtain:

$$r=\frac{\mathbf{kCIaKads[dye]ads}}{\mathbf{1+Kads[dye]_0ads}} \quad \textbf{(3-25)}$$

$$r=\frac{\mathbf{kobsKads[dye]ads}}{\mathbf{1+Kads[dye]0}} \quad \textbf{(3-26)}$$

$$k_{obs}=k_{CIa}$$

where k_{obs} is the photocatalytic reaction rate constant. It depends on the light intensity, mass and nature of the catalyst, and concentration of the electron carrier (O_2 and H_2O_2)[105]. The limitation of the rate of photocatalytic degradation is also attributed to the recombination of photo generated hole-electron pairs. The adsorbed oxygen on the surface of ZnO prevents the recombination process by trapping electrons , as represented in equation (3-27)

$$e^- + O_2(ads) \rightarrow O_2^-(ads) \quad \textbf{(3-27)}$$

[106]indicated a noncompetitive Langmuir-Hinshelwood model for adsorption of oxygen on the surface of ZnO as follows:

$$\therefore r_{O2} \alpha \frac{\mathbf{KO2[O2]}}{\mathbf{1+KO2[O2]}} \quad \textbf{(3-28)}$$

Where K_{O2} is the adsorption equilibrium constant of oxygen, so the equation (3-28) will be as follows:

$$\therefore r_{dye}=\frac{kDKads[dye]ads}{1+Kads[dye]0} \qquad (3\text{-}29)$$

$$\therefore r_{dye}=kap[dye] \qquad (3\text{-}30)$$

$$where\ k_D = \frac{kobsKO2[O2]}{1+KO2[O2]}\ and\ kap= \frac{kDKads}{1+Kads[dye]0}$$

Equation (3-29) shows a pseudo-first order reaction with respect to the dye concentration. From equation (3-29), the values of k_D and K_{ads} were determined for different light intensities .

Integration of equation(3-29) will give:

$$K_{ads}\ k_D t = \ln \frac{C0}{Ct} + Kads(C0 - Ct) \qquad (3\text{-}31)$$

Obviously, equation(3-31) shows the sum of zero-order and first-order rate equations. Their contribution to the overall reaction depends essentially on the initial concentration C_0. When C_0 is very small, equation (3-31)is reduced to equation(3-32):

$$\ln \frac{C0}{Ct} = k_E t \qquad (3\text{-}32)$$

$$k_E = K_{ads} k_D$$

Also the half life time calculated from equation (3-30) could be written as:

$$t= \frac{1}{krKads} \ln \frac{C0}{Ct} + \frac{1}{kr}(C0 - Ct) \qquad (3\text{-}33)$$

Where (t) is the reaction time during degradation of dye from concentration C_0 to C, the half life time of reaction C =0.5C_0, the reaction time of (t) is ($^*t_{½}$), thus the equation (3-33) becomes:

$$^*t_{½} = \frac{0.5C0}{kr} + \frac{\ln 2}{krKads} \qquad (3\text{-}34)$$

Where $^*t_{½}$ half-life time of reactions estimated from theory, equation (3-34) indicates that a plot of $^*t_{½}$ versus the values of initial concentration of dye would be linear by substituting values of Kr and K ads that are obtained from equation (3-22) and are illustrated in Table 4.5. In equation (3-35), the estimated half-lives are obtained. Since half-lives for first-order reaction could also be calculated by applying the last conditions as in equation (3-32):

$$t_{½} = \frac{\ln 2}{k} \qquad (3\text{-}35)$$

where $t^{½}$ is the half –life time of reactions in different concentrations calculated from k which is the observed reaction rate constant for photodegradation of dye in different initial concentrations[107].

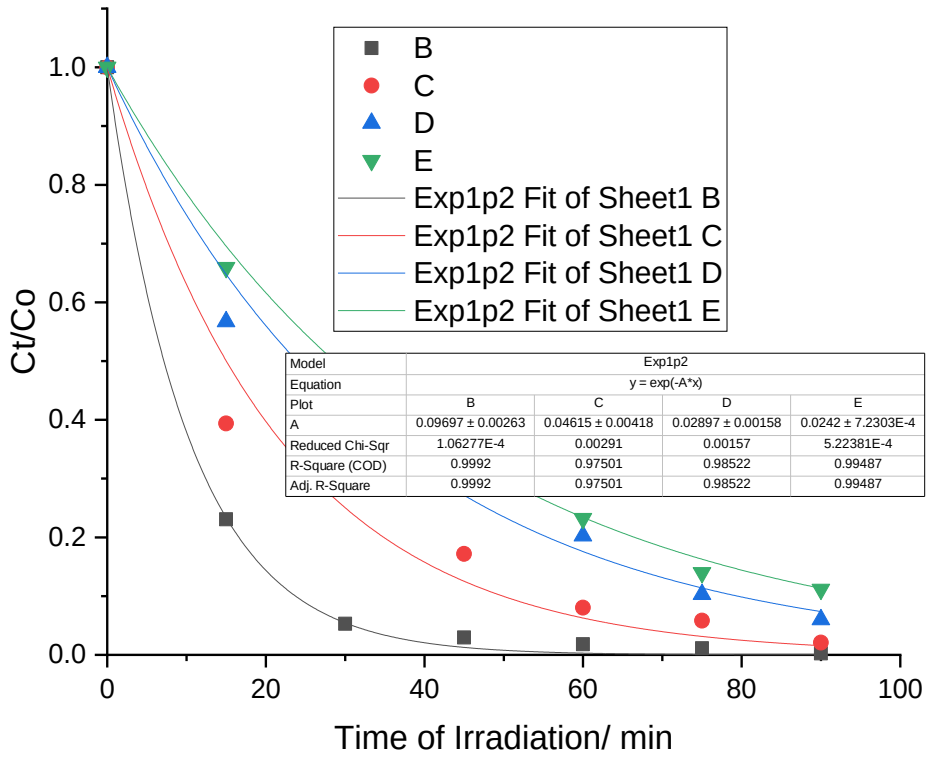

Model	Exp1p2			
Equation	y = exp(-A*x)			
Plot	B	C	D	E
A	0.09697 ± 0.00263	0.04615 ± 0.00418	0.02897 ± 0.00158	0.0242 ± 7.2303E-4
Reduced Chi-Sqr	1.06277E-4	0.00291	0.00157	5.22381E-4
R-Square (COD)	0.9992	0.97501	0.98522	0.99487
Adj. R-Square	0.9992	0.97501	0.98522	0.99487

Figure (3-8): Effect of irradiation time at different concentrations of dye

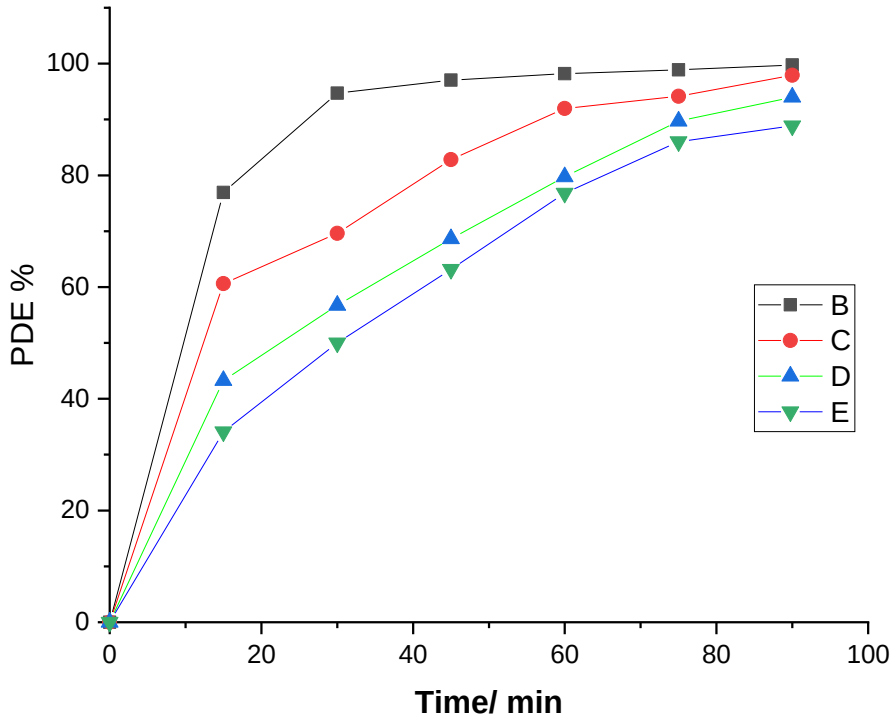

Figure (3-9): Photocatalysis efficiency at different concentrations with time change

3-3 Conclusions:

1. the prepared ZnO show good photocatalytic activity for removal of dyes.

2. silver doped of ZnO shows the highest photocatalysis in our study.

3. When light intensity increased the photodegradation increased.

4. When pollutants concentrations increased the photodegradation decreased.

5. clear shift shows by using DR/ spectrophotometer, means created

Plasmon resonance on the surface of Ag/ZnO

3-4 Suggestions for Further Study

1. Using other metals doping on semiconductors, such as M (Pt. Au, Pd) ZnO, for enhanced optical and photocatalytic properties.
2. Using a new a type of lights as a sources of photo-degradations (solar light and visible light on the M/ZnO surface)
3. Using the prepared surface as a model for antibacterial activity.
4. Using the prepared surface as a source of photo reduction for organic compounds

Reference

1. Manou, L., et al., *What does "Nanoscience–Nanotechnology" mean to primary school teachers?* International Journal of Science and Mathematics Education, 2021: p. 1-22.

2. Taniguchi, N., *On the basic concept of nano-technology proceedings of the international conference on production engineering tokyo part ii japan society of precision engineering.* Pabbati et al, 1974.

3. Bayda, S., et al., *The history of nanoscience and nanotechnology: From chemical–physical applications to nanomedicine.* Molecules, 2020. **25**(1): p. 112.

4. Mazari, S.A., et al., *Nanomaterials: Applications, waste-handling, environmental toxicities, and future challenges–A review.* Journal of Environmental Chemical Engineering, 2021. **9**(2): p. 105028.

5. Sannino, D., *Types and Classification of Nanomaterials*, in *Nanotechnology*. 2021, Springer. p. 15-38.

6. Rohilla, D., S. Chaudhary, and A. Umar, *An overview of advanced nanomaterials for sensor applications.* Engineered Science, 2021. **16**: p. 47-70.

7. Salem, S.S., et al., *A Comprehensive Review of Nanomaterials: Types, Synthesis, Characterization, and Applications.* 2022.

8. Baig, N., I. Kammakakam, and W. Falath, *Nanomaterials: A review of synthesis methods, properties, recent progress, and challenges.* Materials Advances, 2021. **2**(6): p. 1821-1871.

9. Alkaç, İ.M., et al., *Nanomaterials and their classification*, in *Nanomaterials for Direct Alcohol Fuel Cells*. 2021, Elsevier. p. 17-33.

10. Saleh, T.A., *Nanomaterials: Classification, properties, and environmental toxicities.* Environmental Technology & Innovation, 2020. **20**: p. 101067.

11. Kolahalam, L.A., et al., *Review on nanomaterials: Synthesis and applications.* Materials Today: Proceedings, 2019. **18**: p. 2182-2190.

12. Liu, J.L. and S. Bashir, *Advanced nanomaterials and their applications in renewable energy.* 2015.

13. Syah, R., et al., *CuMoO4/ZnO Nanocomposites: Novel Synthesis, Characterization, and Photocatalytic Performance.* Journal of Nanostructures, 2021. **11**(1): p. 73-80.

14. Noah, N.M., *Design and synthesis of nanostructured materials for sensor applications.* Journal of Nanomaterials, 2020. **2020**.

15. Mousavi, S.M., et al., *Shape-controlled synthesis of zinc nanostructures mediating macromolecules for biomedical applications.* Biomaterials Research, 2022. **26**(1): p. 1-20.

16. De Corrado, J.M., et al., *ZnO colloid crystal facet-type determines both Au photodeposition and photocatalytic activity.* ACS Applied Nano Materials, 2019. **2**(12): p. 7856-7869.

17. Nadupalli, S., et al., *About defect phenomena in ZnO nanocrystals.* Nanoscale, 2021. **13**(20): p. 9160-9171.

18. Wang, Z., M.R. Bockstaller, and K. Matyjaszewski, *Synthesis and applications of ZnO/polymer nanohybrids.* ACS Materials Letters, 2021. **3**(5): p. 599-621.

19. Koe, W.S., et al., *An overview of photocatalytic degradation: photocatalysts, mechanisms, and development of photocatalytic membrane.* Environmental Science and Pollution Research, 2020. **27**(3): p. 2522-2565.

20. Rahman, F., *Zinc oxide light-emitting diodes: a review.* Optical Engineering, 2019. **58**(1): p. 010901.

21. Ahmad, M.P., et al., *Particle size effect on the dielectric properties of ZnO nanoparticles.* Materials Chemistry and Physics, 2019. **224**: p. 79-84.

22. Bharat, T., et al., *Synthesis of doped zinc oxide nanoparticles: a review.* Materials Today: Proceedings, 2019. **11**: p. 767-775.

23. Kumar, S., et al., *Nanoscale zinc oxide based heterojunctions as visible light active photocatalysts for hydrogen energy and environmental remediation.* Catalysis Reviews, 2020. **62**(3): p. 346-405.

24. Vyas, S., *A short review on properties and applications of ZnO based thin film and devices.* Johnson Matthey Technology Review, 2020.

25. Yang, G. and S.-J. Park, *Conventional and microwave hydrothermal synthesis and application of functional materials: A review.* Materials, 2019. **12**(7): p. 1177.

26. Mamaghani, A.H., F. Haghighat, and C.-S. Lee, *Hydrothermal/solvothermal synthesis and treatment of TiO2 for photocatalytic degradation of air pollutants: Preparation, characterization, properties, and performance.* Chemosphere, 2019. **219**: p. 804-825.

27. Ye, N., et al., *A review: conventional and supercritical hydro/solvothermal synthesis of ultrafine particles as cathode in lithium battery.* Ceramics International, 2018. **44**(5): p. 4521-4537.

28. Pimentel, A., et al., *Effect of solvents on ZnO nanostructures synthesized by solvothermal method assisted by microwave radiation: A photocatalytic study.* Journal of Materials Science, 2015. **50**(17): p. 5777-5787.

29. Zhao, J., et al., *The NiO electrode materials in electrochemical capacitor: A review.* Materials Science in Semiconductor Processing, 2019. **96**: p. 78-90.

30. Li, S.-M., et al., *Acetone sensing of ZnO nanosheets synthesized using room-temperature precipitation.* Sensors and Actuators B: Chemical, 2017. **249**: p. 611-623.

31. Sundar, K.P. and S. Kanmani, *Progression of Photocatalytic reactors and it's comparison: A Review.* Chemical Engineering Research and Design, 2020. **154**: p. 135-150.

32. Long, Z., et al., *Historical development and prospects of photocatalysts for pollutant removal in water.* Journal of hazardous materials, 2020. **395**: p. 122599.

33. Weldegebrieal, G.K., *Synthesis method, antibacterial and photocatalytic activity of ZnO nanoparticles for azo dyes in wastewater treatment: A review.* Inorganic Chemistry Communications, 2020. **120**: p. 108140.

34. Prasad, A.R., et al., *Applications of phytogenic ZnO nanoparticles: A review on recent advancements.* Journal of Molecular Liquids, 2021. **331**: p. 115805.

35. Akerdi, A.G. and S.H. Bahrami, *Application of heterogeneous nano-semiconductors for photocatalytic advanced oxidation of organic compounds: a review.* Journal of Environmental Chemical Engineering, 2019. **7**(5): p. 103283.

36. H Abdulrazzak, F., et al., *Antimicrobial Activity of Ag: ZnO/MWCNT against Acinetobacter baumannii.* Journal of Nanostructures, 2021. **11**(2): p. 317-322.

37. Rahman, A., et al., *Zinc oxide and zinc oxide-based nanostructures: biogenic and phytogenic synthesis, properties and applications.* Bioprocess and Biosystems Engineering, 2021. **44**(7): p. 1333-1372.

38. Malini, B. and G.A.G. Raj, *PREPARATION AND SOLAR ASSISTED PHOTOCATALYTIC PERFORMANCE OF AG-DOPED ZNO FOR ROSE BENGAL DYE DEGRADATION.* 2022.

39. Hashim, F.S., et al., *Effect of (Ag, Pd) doping on structural, and optical properties of ZnO nanoparticales: As a model of photocatalytic activity for water pollution treatment.* Chemical Physics Letters, 2019. **737**: p. 136828.

40. Liu, Y., et al., *Novel and efficient synthesis of Ag-ZnO nanoparticles for the sunlight-induced photocatalytic degradation.* Applied Surface Science, 2019. **476**: p. 632-640.

41. Messih, M.A., et al., *Synthesis and characterization of novel Ag/ZnO nanoparticles for photocatalytic degradation of methylene blue under UV and solar irradiation.* Journal of Physics and Chemistry of Solids, 2019. **135**: p. 109086.

42. Ullattil, S.G., M. Jabeen Fatima, and A. Abdel-Wahab, *Defect minimized Ag-ZnO microneedles for photocatalysis.* Environmental Science and Pollution Research, 2020. **27**(29): p. 37036-37043.

43. Jing, L., et al., *The surface properties and photocatalytic activities of ZnO ultrafine particles.* Applied Surface Science, 2001. **180**(3-4): p. 308-314.

44. KinuyoKawano, M., YoshiyukiYajima, HajimeHaneda, HideyukiMaki, TaiseiYamamoto, *Photoreduction of Ag ion on ZnO single crystal.* Applied surface science, 2002. **189**: p. 265-270.

45. Gokon, N., et al., *Photocatalytic effect of ZnO on carbon gasification with CO2 for high temperature solar thermochemistry.* Solar energy materials and solar cells, 2003. **80**(3): p. 335-341.

46. Liqiang, J., Baifu Xin,Fulong Yuan,Baiqi Wang,Keying Shi,WeiminCai,Honggang Fu, *Deactivation and regeneration of ZnO and TiO2 nanoparticles in the gas phase photocatalytic oxidation of n-C7H16 or SO2.* Applied Catalysis A: General, 2004. **275**: p. 49-54.

47. Hsu Chin-Cheng, W.N.-L., *Synthesis and photocatalytic activity of ZnO/ZnO2 composite.* Journal of Photochemistry and Photobiology A: Chemistry, 2005. **172**: p. 269-274.

48. Height Murray J, P.S.E., Mekasuwandumrong Okorn,Praserthdam Piyasan, *Ag-ZnO catalysts for UV-photodegradation of methylene blue.* Applied Catalysis B: Environmental, 2006. **63**: p. 305-312.

49. Vladimir K. Ivanov , S.A.S., Sharikov Felix Yu ,Baranchikov Alexander Ye, *Hydrothermal and microwave-assisted synthesis of nanocrystalline ZnO photocatalysts.* Superlattices and Microstructures, 2007. **42**: p. 421-424.

50. Tan Tian, L.Y., Liu Yi,Wang Bo,Song Xuemei,Li Er,Wang Hao,Yan Hui,, *Two-step preparation of Ag/tetrapod-like ZnO with photocatalytic activity by thermal evaporation and sputtering.* Materials Chemistry and Physics, 2008. **111**: p. 305-308.

51. Mohajerani, M.S., A. Lak, and A. Simchi, *Effect of morphology on the solar photocatalytic behavior of ZnO nanostructures.* Journal of alloys and compounds, 2009. **485**(1-2): p. 616-620.

52. Wu, D., et al., *One step from ZnO rod to ZnS porous tube.* Materials Science and Engineering: B, 2010. **175**(3): p. 195-200.

53. Qamar, M., M. Gondal, and Z. Yamani, *Laser-induced efficient reduction of Cr (VI) catalyzed by ZnO nanoparticles.* Journal of hazardous materials, 2011. **187**(1-3): p. 258-263.

54. Giraldi, T.R., et al., *Effect of synthesis parameters on the structural characteristics and photocatalytic activity of ZnO.* Materials Chemistry and Physics, 2012. **136**(2-3): p. 505-511.

55. Wei, A., et al., *One-step electrochemical synthesis of a graphene–ZnO hybrid for improved photocatalytic activity*. Materials Research Bulletin, 2013. **48**(8): p. 2855-2860.

56. Pan, L., et al., *Undoped ZnO abundant with metal vacancies.* Nano Energy, 2014. **9**: p. 71-79.

57. Manna, J., et al., *Photocatalytic hybrid Au/ZnO nanoparticles assembled through a one-pot method.* Journal of colloid and interface science, 2015. **460**: p. 113-118.

58. Ding, D., et al., *A simple method for preparing ZnO foam/carbon quantum dots nanocomposite and their photocatalytic applications.* Materials Science in Semiconductor Processing, 2016. **47**: p. 25-31.

59. Man, M.T., et al., *Oriented ZnO nanostructures and their application in photocatalysis.* Journal of luminescence, 2017. **185**: p. 17-22.

60. Kimiagar, S., S. Safa, and S. Gharedaghi, *N-doped graphene: a trustful additive concerning to the photocatalytic properties of ZnO*. Optik, 2018. **174**: p. 163-166.

61. Soto-Robles, C., et al., *Study on the effect of the concentration of Hibiscus sabdariffa extract on the green synthesis of ZnO nanoparticles.* Results in Physics, 2019. **15**: p. 102807.

62. Chen, C., et al., *Synthesis of a flower-like SnO/ZnO nanostructure with high catalytic activity and stability under natural sunlight.* Journal of Alloys and Compounds, 2020. **826**: p. 154122.

63. Le Pivert, M., et al., *ZnO nanostructures based innovative photocatalytic road for air purification.* Journal of Cleaner Production, 2021. **318**: p. 128447.

64. Muñoz-Fernandez, L., et al., *Influence of nanoscale defects on the improvement of photocatalytic activity of Ag/ZnO*. Materials Characterization, 2022. **185**: p. 111718.

65. Khan, H., et al., *Experimental methods in chemical engineering: X-ray diffraction spectroscopy—XRD.* The Canadian Journal of Chemical Engineering, 2020. **98**(6): p. 1255-1266.

66. Ameh, E., *A review of basic crystallography and x-ray diffraction applications.* The international journal of advanced manufacturing technology, 2019. **105**(7): p. 3289-3302.

67. Holder, C.F. and R.E. Schaak, *Tutorial on powder X-ray diffraction for characterizing nanoscale materials*. 2019, ACS Publications. p. 7359-7365.

68. Havrdova, M., et al., *Field emission scanning electron microscopy (FE-SEM) as an approach for nanoparticle detection inside cells.* Micron, 2014. **67**: p. 149-154.

69. Barbay, C., et al., *Dislocations imaging in low boron doped diamond epilayers using Field Emission Scanning Electron Microscopy (FE-SEM).* Applied Surface Science, 2019. **495**: p. 143564.

70. Cerqueira, B., et al., *Using time of flight secondary ion mass spectrometry and field emission scanning electron microscopy with energy dispersive X-ray spectroscopy to determine the role of soil components in competitive copper and cadmium migration and fixation in soils.* Geoderma, 2015. **251**: p. 65-77.

71. Yang, R., et al., *Nano-scale pore structure and fractal dimension of organic-rich Wufeng-Longmaxi shale from Jiaoshiba area, Sichuan Basin: Investigations using FE-SEM, gas adsorption and helium pycnometry.* Marine and Petroleum Geology, 2016. **70**: p. 27-45.

72. Spurgeon, S.R., et al., *Towards data-driven next-generation transmission electron microscopy.* Nature materials, 2021. **20**(3): p. 274-279.

73. Rocha, F.S., et al., *Experimental methods in chemical engineering: Ultraviolet visible spectroscopy—UV-Vis.* The Canadian Journal of Chemical Engineering, 2018. **96**(12): p. 2512-2517.

74. Makuła, P., M. Pacia, and W. Macyk, *How to correctly determine the band gap energy of modified semiconductor photocatalysts based on UV–Vis spectra*. 2018, ACS Publications. p. 6814-6817.

75. M. Zhou, Lv, W., Liu, C., Liu, D., and Wang, Y., *Flower-like and hollow sphere-like ZnO assisted by microorganisms and their UV absorption and photo catalytic performance.* Journal of Materials Science: Materials in Electronics, 2013. **24**(1): p. 36-43.

76. X. Wang, Zhang, Y., Hao, C., Feng, F., Yin, H., Si, N., *Solid-Phase Synthesis of Mesoporous ZnO Using Lignin-Amine Template and Its Photocatalytic Properties.* Industrial and Engineering Chemistry Research, 2014. **53**(16): p. 6585-6592.

77. Zhu, X., et al., *Fabrication, characterization and high photocatalytic activity of Ag–ZnO heterojunctions under UV-visible light.* RSC advances, 2021. **11**(44): p. 27257-27266.

78. Benhebal, H., et al., *Photocatalytic degradation of phenol and benzoic acid using zinc oxide powders prepared by the sol–gel process.* Alexandria Engineering Journal, 2013. **52**(3): p. 517-523.

79. Chauhan, P.S., et al., *Facile synthesis of ZnO/GO nanoflowers over Si substrate for improved photocatalytic decolorization of MB dye and industrial wastewater under solar irradiation.* Materials science in semiconductor processing, 2019. **89**: p. 6-17.

80. Sáaedi, A., et al., *Optical and electrical properties of p-type Li-doped ZnO nanowires.* Superlattices and Microstructures, 2013. **61**: p. 91-96.

81. Ibănescu, M., et al., *Photocatalytic and antimicrobial Ag/ZnO nanocomposites for functionalization of textile fabrics.* Journal of Alloys and Compounds, 2014. **610**: p. 244-249.

82. Choi, Y.I., et al., *Band gap-engineered ZnO and Ag/ZnO by ball-milling method and their photocatalytic and Fenton-like photocatalytic activities.* Applied Surface Science, 2015. **356**: p. 615-625.

83. Muñoz-Fernandez, L., et al., *Solvothermal synthesis of Ag/ZnO and Pt/ZnO nanocomposites and comparison of their photocatalytic behaviors on dyes degradation.* Advanced Powder Technology, 2016. **27**(3): p. 983-993.

84. Abbas, A.M., et al. *Photocatalytic activity of Ag-ZnO nanocomposites integrated essential ginger oil fabricated by green synthesis method*. in *Journal of Physics: Conference Series*. 2021. IOP Publishing.

85. Huang, Q., et al., *Selective synthesis of different ZnO/Ag nanocomposites as surface enhanced Raman scattering substrates and highly efficient photocatalytic catalysts.* RSC Advances, 2015. **5**(34): p. 27075-27081.

86. Pham, T.T.H., et al., *Ag nanoparticles on ZnO nanoplates as a hybrid SERS-active substrate for trace detection of methylene blue.* RSC advances, 2022. **12**(13): p. 7850-7863.

87. Jaramillo-Páez, C., et al., *High UV-photocatalytic activity of ZnO and Ag/ZnO synthesized by a facile method.* Catalysis Today, 2017. **284**: p. 121-128.

88. Tabatabaee, M. and S.A. Mirrahimi, *Photodegradation of dye pollutant on Ag/ZnO Nanocatalyst under UV-irradiation.* Oriental Journal of Chemistry, 2011. **27**(1): p. 65.

89. Shanker, U., M. Rani, and V. Jassal, *Degradation of hazardous organic dyes in water by nanomaterials.* Environmental chemistry letters, 2017. **15**(4): p. 623-642.

90. Gouthaman, A., et al., *Enhanced dye removal using polymeric nanocomposite through incorporation of Ag doped ZnO nanoparticles: Synthesis and characterization.* Journal of hazardous materials, 2019. **373**: p. 493-503.

91. Jamal, M.A., M. Muneer, and M. Iqbal, *Photo-degradation of monoazo dye blue 13 using advanced oxidation process.* Chem. Int, 2015. **1**(1): p. 12-16.

92. Chiu, Y.-H., et al., *Mechanistic insights into photodegradation of organic dyes using heterostructure photocatalysts.* Catalysts, 2019. **9**(5): p. 430.

93. Lam, S.-M., J.-A. Quek, and J.-C. Sin, *Mechanistic investigation of visible light responsive Ag/ZnO micro/nanoflowers for enhanced photocatalytic performance and antibacterial activity.* Journal of Photochemistry and Photobiology A: Chemistry, 2018. **353**: p. 171-184.

94. Guo, Y., et al., *Efficient green photocatalyst of Ag/ZnO nanoparticles for methylene blue photodegradation.* Journal of Materials Science: Materials in Electronics, 2022. **33**(5): p. 2716-2728.

95. Kanwal, M., S.R. Tariq, and G.A. Chotana, *Photocatalytic degradation of imidacloprid by Ag-ZnO composite.* Environmental Science and Pollution Research, 2018. **25**(27): p. 27307-27320.

96. Wang, H., X. Liu, and S. Han, *The synthesis of a Ag–ZnO nanohybrid with plasmonic photocatalytic activity under visible-light irradiation: the relationship between tunable optical absorption, defect chemistry and photocatalytic activity.* CrystEngComm, 2016. **18**(11): p. 1933-1943.

97. Behnajady, M., N. Modirshahla, and R. Hamzavi, *Kinetic study on photocatalytic degradation of CI Acid Yellow 23 by ZnO photocatalyst.* Journal of hazardous materials, 2006. **133**(1-3): p. 226-232.

98. Rao, A.N., B. Sivasankar, and V. Sadasivam, *Kinetic studies on the photocatalytic degradation of Direct Yellow 12 in the presence of ZnO catalyst.* Journal of molecular catalysis A: Chemical, 2009. **306**(1-2): p. 77-81.

99. Daneshvar, N., et al., *Preparation and investigation of photocatalytic properties of ZnO nanocrystals: effect of operational parameters and kinetic study.* evaluation, 2007. **900**: p. 6.

100. Kim, S., et al., *A kinetic study of ZnO atomic layer deposition: Effects of surface hydroxyl concentration and steric hindrance.* Applied Surface Science, 2019. **469**: p. 804-810.

101. Rajabi, M., K. Mahanpoor, and O. Moradi, *Thermodynamic and kinetic studies of crystal violet dye adsorption with poly (methyl methacrylate)–graphene oxide and poly (methyl methacrylate)–graphene oxide–zinc oxide nanocomposites.* Journal of Applied Polymer Science, 2019. **136**(22): p. 47495.

102. Aggarwal, S. and S. Ikram, *Zinc oxide nanoparticles-impregnated chitosan surfaces for covalent immobilization of trypsin: Stability & kinetic studies.* International Journal of Biological Macromolecules, 2022. **207**: p. 205-221.

103. Tekin, D., H. Kiziltas, and H. Ungan, *Kinetic evaluation of ZnO/TiO2 thin film photocatalyst in photocatalytic degradation of Orange G.* Journal of Molecular Liquids, 2020. **306**: p. 112905.

104. Bafghi, M.S., M. Karimi, and M. Adeli, *A kinetic study on the carbothermic reduction of zinc oxide from electric arc furnace dust.* Iranian Journal of Materials Science and Engineering, 2013. **10**(4): p. 18-30.

105. David, C.A., et al., *Dissolution kinetics and solubility of ZnO nanoparticles followed by AGNES.* The Journal of Physical Chemistry C, 2012. **116**(21): p. 11758-11767.

106. Bilecka, I., P. Elser, and M. Niederberger, *Kinetic and thermodynamic aspects in the microwave-assisted synthesis of ZnO nanoparticles in benzyl alcohol.* ACS nano, 2009. **3**(2): p. 467-477.

107. Zhang, J., et al., *Kinetics studies of dimethyl carbonate synthesis from urea and methanol over ZnO catalyst.* Korean Journal of Chemical Engineering, 2010. **27**(6): p. 1744-1749.

الخلاصة

في هذه الدراسة, تم تحضر اوكسيد الزنك باستخدام تقنية المذيب الحرارية عند درجة حرار 37̊c, ,عند الدالة الحامضية 6 وتم حرق العينات لمدة (ساعة) عند درجة حرارة (500̊c) . كذالك تم تحضير (Ag-ZnO) بطريقة الترسيب الضوئي باستخدام الاشعة فوق البنفسجية.

تم تشخص الخصائص الكيميائية والفيزيائية للمركبات النانوية المحضره باستخدام تقنيات مختلفة مثل انحراف الشعة السينية (XRD) ,المجهر الالكتروني النافذ (TEM) ,المجهر الالكتروني الماسح (SEM) والاشعة فوق البنفسجية – المرئية .اظهرت نتائج SEM, TEM وجود تكتلات عالية ZnO ونسبة قليلة من Ag على سطح ZnO , لذالك لم تظهر نتائج XRD اي قمم الى Ag . اظهرت تقنية الاشعة فوق البنفسجية –المرئية ان فجوة الطاقة الاوكسيد الزنك اختزلت واصبحت اقل بعد اضافة الفضة .

تم دراسة التفكك الضوئي لصبغة Brilliant green باستعمال اللاشعة فوق البنفسجية تحت ظروف مختلافة في وجود Ag-ZnO , دراسة تأثير بعض العوامل مثل تاثير تركيز الصبغة ,شدة الضوء الساقط ودراسة تاثير الزمن .

اظهرات النتائج ان كفاءة التحطيم للسطح اوكسيد الزنك انها تزداد 92.8% بعد اضافة الفضة. كما أظهر أن معدل التحطم التحفيزي الضوئي يزداد مع تناقص تركيز صبغة.Brilliant green و أدت زيادة شدة الضوء إلى زيادة معدل التحطم التحفيزي الضوئي .

اظهرات نتائج هذه الدراسة ان تفاعلات التجزئة الضوئيه للصبغة المرتبة الاولى الكاذبة.

وزارة التعليم العالي والبحث العلمي

جامعة بابل / كلية العلوم للبنات

قسم الكيمياء

دراسة الفاعلية الضوئية المحفزة ZnO و M/ZnO :كنموذج لدراسة المقارنة

رسالة مقدمة إلى

مجلس كليــة العلوم للبنات في جامعــة بابــل وهي جـزء من
متطلبات نيل درجــة الماجستير في الكيمياء

مقدمة من قبل

نور قصي عبد الصاحب جاسم بيدنو

بكالوريوس في الكيمياء
جامعة بابل /كلية العلوم للبنات (٢٠١٨-٢٠١٩) م

بإشراف

أ.د اياد فاضل القيم

١٤٤٣هـ ٢٠٢٢م